# Global LPV model identification of flapping-wing dynamics using flight data

Armanini, Sophie; Karasek, Matej; de Visser, Coen

**Important note**
To cite this publication, please use the final published version (if applicable).
Please check the document version above.

# Global LPV model identification of flapping-wing dynamics using flight data

S.F. Armanini[*], M. Karásek [†], C.C. de Visser[‡]

*Delft University of Technology, 2629HS Delft, The Netherlands.*

Biologically-inspired flapping-wing micro aerial vehicles are characterised by nonlinear, unsteady aerodynamics and complex dynamics, both highly challenging to model. To take full advantage of the flight capabilities of such vehicles, it is necessary to obtain insight into their dynamics in the different flyable conditions, and to provide adequate control in all of these conditions. Nonetheless, the dynamics are typically only considered in a single flight regime, and controllers are frequently tuned for a particular flight condition. Due the high complexity of flapping flight and limited availability of accurate free-flight data, global models are not yet readily available, particularly models based on free-flight data and suitable for practical applications. This paper demonstrates an approach to obtain a global dynamic model for a flapping-wing micro aerial vehicle. To allow for standard linear control and systems theory to be applied, the nonlinear dynamics are approximated using a linear parameter-varying (LPV) approach based on a set of local linear models. The scheduling parameters, and the parameters in the underlying local models, are determined using system identification methods applied to free-flight data collected on a real test platform, and covering a significant part of the flight envelope. The proposed approach allows for modelling of the vehicle and prediction of the dominant dynamic properties across the considered part of the flight envelope, using a total of 16 parameters, as opposed to the starting point of 46 local models with 12 parameters each. The use of a single model adapting to the flight condition provides flexibility and continuous coverage, and is therefore highly useful for simulation and control applications. While in the explored part of the flight envelope the nonlinearity was found to be limited, such that a weighted average model may be sufficient for some applications, the LPV model provides a higher accuracy and more consistent performance across the conditions considered. Additionally, the approach is shown to be promising and is expected to be adaptable to cover more significant variation. Improvements could be obtained through more extensive flight envelope coverage, more accurate measurement and more informative identification data.

## I.  Introduction

Flapping-wing micro aerial vehicles (FWMAVs) are attracting an ever-increasing interest from the aerospace community. Inspired by natural flyers, they can achieve outstanding manoeuvrability, agility and efficiency, at very small scales and low flight velocities. Thanks to their unique properties, FWMAVs are expected to fill in the gap between fixed-wing and rotating-wing vehicles, allowing for unprecedented performance, particularly for flight indoors or in complex cluttered environments. Despite the significant progress that has been made in understanding flapping-wing mechanisms,[1,2,3,4,5,6] however, FWMAVs remain challenging to model, due to their unsteady aerodynamics and complex time-varying dynamics.

One particular challenge is to obtain models covering different flight conditions. Particularly low-order models of flapping-wing dynamics and aerodynamics typically have a limited applicability range and/or have not been validated in different conditions with free-flight data.[7,8,9,10,11,12,13,14] However, it is essential to

---

[*]PhD Student, Control & Simulation Section, Faculty of Aerospace Engineering, Kluyverweg 1, 2629HS Delft, The Netherlands. s.f.armanini@tudelft.nl. AIAA Student Member.

[†]Postdoctoral Researcher, Control & Simulation Section, Faculty of Aerospace Engineering, Kluyverweg 1, 2629HS Delft, The Netherlands.

[‡]Assistant Professor, Control & Simulation Section, Faculty of Aerospace Engineering, Kluyverweg 1, 2629HS Delft, The Netherlands. AIAA Member.

know how a system behaves in all its operating conditions, in order to ensure an effective operation and maximise its performance. Furthermore, accurate global models are highly valuable and often indispensable to provide more realistic and comprehensive simulation possibilities, support the development and testing of new controllers and allow for the application of more advanced control approaches. A limited validity domain is particularly constraining in the flapping-wing case, because FWMAVs can typically operate in different regimes, which can lead to significantly different flight properties.

In the context of control and simulation, an additional challenge is that models must be not only accurate, and ideally validated with free-flight data, but also computationally efficient and suitable for practical application. Hence, simplified models are preferable when they can achieve sufficient accuracy. When flight data are available, an alternative to typically complex and computationally expensive numerical or first-principles models is therefore system identification. This approach is not yet widespread due to the difficulty of obtaining suitable data, nonetheless existing work[7,15,16,17,8,9,18] has shown that it can yield models that are at the same time realistic, relatively simple and applicable in the context of control and simulation.

This paper addresses the challenge of global data-driven modelling of flapping-wing vehicles, using the example of an existing, flight-capable FWMAV, the DelFly II.[19] Starting from flight data, we identify a model of the cycle-averaged vehicle dynamics that covers a range of different flight conditions, representing a significant part of the flight envelope achievable by the vehicle in a single configuration. Based on a preliminary analysis of the data and on local modelling results, the global dynamics are approximated using a linear parameter-varying (LPV) modelling approach, starting from a set of local linear time-invariant (LTI) models. LPV modelling is closely related to gain-scheduling control, and is based on the idea that a global model (or a model covering all operating conditions) can be obtained by interpolating between local models (or models valid at specific operating conditions), which are typically linear.[20,21,22] The LPV approach represents an attractive global modelling solution, avoiding complex high-order model structures, and also typically results in global models that are compatible with established linear control methods. LPV control and modelling methods have been applied to a variety of dynamic systems, including aircraft,[23,24,25,26,27,28,29,30] but not yet to FWMAVs. Hence, in addition to the primary aim of developing an accurate low-order global model for a specific FWMAV, the current study also represents an investigation into the applicability of an LPV approach to model flapping-wing dynamics.

Given that no first principles model of the test platform is available, we opt for an identification approach, involving two steps: firstly, local linear models are identified from free-flight data collected on the vehicle; secondly, a set of interpolating functions are determined to combine these models into a global LPV model. Potential scheduling variables are selected based on analysis of the collected flight data and of the local models, while the scheduling functions defining the global model are determined using stepwise regression.[31] The resulting global model is evaluated through comparison with both flight data and local models, in conditions where local models and data are available. To evaluate the robustness and reliability of the results, evaluations are also performed using validation data that were not used in the estimation process.

This paper is organised as follows. Section II describes the test vehicle and experimental data used in this study. Section III introduces the local models at the basis of the global modelling approach, and briefly evaluates both these models and the flight data, focusing on the observations relevant for the subsequent global modelling. Section IV outlines the LPV modelling approach used to transition from the local models to the global models and discusses the scheduling results and final model structure adjustments. Section V presents the main results and evaluates the obtained LPV model in comparison to flight data. Section VI summarises the main conclusions drawn.

## II.    Methods and experimental data

### II.A.    Test vehicle

The subject of this study is a four-winged FWMAV[19] (cf. Fig. 1) with a 280mm wing span, typical flapping frequencies in the range of 10-15Hz and a flight envelope ranging from near hover to fast forward flight. While flight speeds up to 7m/s have been achieved by shifting the CG position through physically moving parts of the payload (e.g. the battery), the flight speeds achievable in the typical configuration range from near hover to approximately 1.5m/s. The mylar foil wings have an 'X'-configuration, allowing for increased lift production thanks to the clap-and-peel effect. The T-shaped styrofoam tail leads to static stability and separates the bulk of the manoeuvring from the wing flapping, such that conventional fixed-wing control mechanisms, based on movable elevator and rudder surfaces, can be used. The same type of vehicle has been

the subject of extensive previous research and detailed geometric properties and descriptions of the design can be found in Ref. 19. Fig. 1(b) shows the definition of the body-fixed coordinate system used throughout this manuscript, which is centred at the centre of gravity (CG) of the vehicle. In contrast to convention, the $z$-axis was defined to be aligned with the fuselage in order to avoid attitude singularities due to the typically large ($> 60°$) pitch angle assumed in flight by this FWMAV.
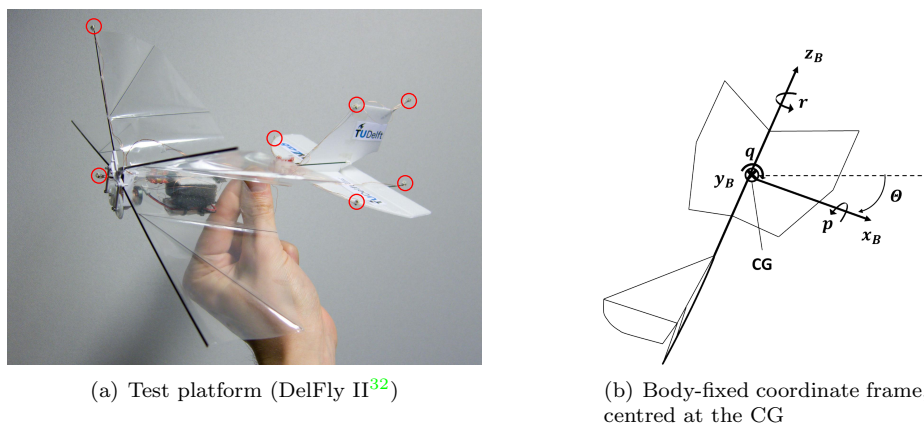


(a) Test platform (DelFly II[32])



(b) Body-fixed coordinate frame, centred at the CG

**Figure 1:** Test platform used in this study and body-fixed coordinate system $x_B, y_B, z_B$

**Table 1:** Mass and inertia properties of the test platform.

| Property | Value |
|---|---|
| $m[kg]$ | 0.0235 |
| $x_{CG}[m]$ (below fuselage) | 0.0096 |
| $y_{CG}[m]$ | 0 |
| $z_{CG}[m]$ (from wing leading edge) | - 0.0695 |
| $I_{xx}, I_{yy}, I_{zz}[Nm^2]$ | 7.5E-05, 6.6E-05, 1.9E-05 |
| $I_{xy}, I_{yz}, I_{xz}[Nm^2]$ | 0, 0, 8.5E-06 |

## II.B.   Flight data acquisition

The modelling work discussed in this paper was based on a set of flight data collected for system identification purposes on the test vehicle described in Sec. II.A. The data were collected using an motion tracking system (24 OptiTrack Flex13 cameras, covering a 10m×10m×7m motion tracking facility) in combination with an on-board inertial measurement unit (IMU) attached to the vehicle. The tracking system was used to measure the positions of seven active LED markers attached to the vehicle at the positions shown in Fig. 1(a), allowing for the reconstruction of body position and orientation, control surface deflections and wing leading edge movement, all at a frequency of 120Hz. The 6-axis IMU, incorporated in the vehicle's Lisa/S autopilot, was used to measure linear accelerations and angular velocities at a frequency of 512Hz. A sensor fusion approach based on extended Kalman filtering was applied to combine the different measurements, leading to high-accuracy and high-resolution measurements.[33] Flight tests were intended for identification of the longitudinal dynamics, and involved elevator input signals, executed by the autopilot when triggered by the pilot.[34] The hardware and flight test setup, data processing and sensor fusion process are described in more detail in Refs. 35 and 34 – the basic process was analogous for this study, however new tests were conducted involving a larger number of manoeuvres, and incorporating minor practical improvements based on the previous flight test campaigns.[35, 34]

## II.C.   Flight test data

In line with aerospace convention, the flight envelope was initially defined in terms of possible combinations of angle of attack (AOA) and velocity. Additionally, the flapping frequency was considered as a further

American Institute of Aeronautics and Astronautics

important variable. This could be considered an additional state, defining the flight envelope together with the AOA and velocity, but could also be seen as an input, as in the test vehicle it is almost entirely a controlled variable, controlled via the motor RPM.[34] Flight test conditions were selected on the basis of previous tests on the same platform,[34,36] and covered trim velocities ranging approximately from 0.5 to 1.3m/s, trim angles of attack (AOA) in the range of 40 to 80°, and flapping frequencies between 10 and 14Hz (cf. Fig. 2). While in absolute terms the covered range is limited, particularly in terms of the velocities covered, in fact this range represents a significant part of the flight envelope achievable with the test vehicle in its current configuration. CG shifts, obtained by moving parts of the hardware (e.g. battery, wings),[36] can be used to further enlarge the flight envelope. However, in view of the restricted test flight space, and because the current work constitutes primarily an investigation into the modelling methodology, no CG shifts were considered in this study. Furthermore, flight testing showed that significant changes in the flight behaviour are already noticeable within the aforementioned range. In total, 46 short (2-5s) manoeuvres for system identification were recorded.
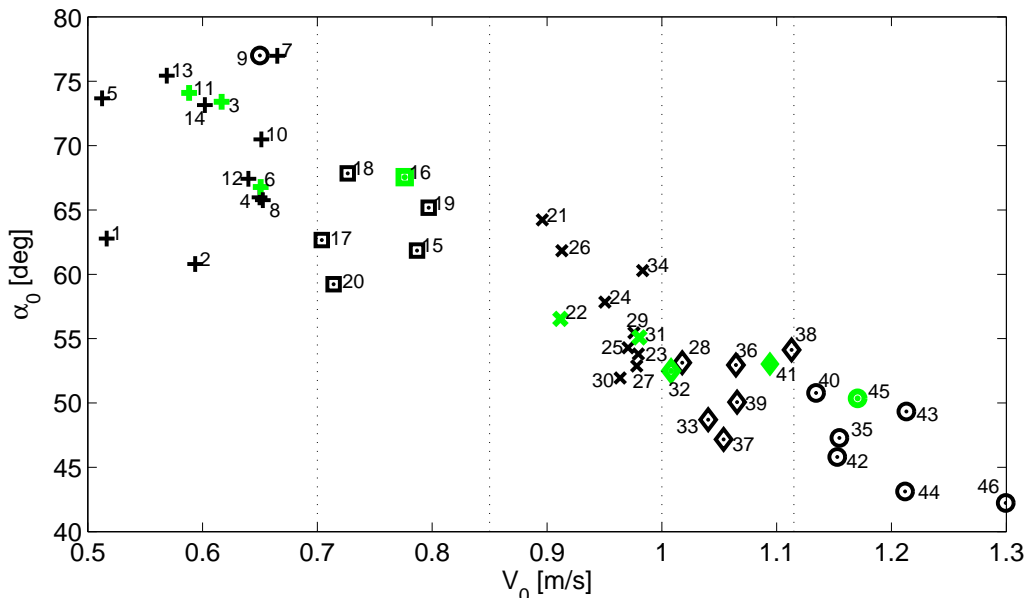


**Figure 2:** Trim conditions for each of the 46 datasets analysed in this study (angle of attack, $\alpha_0$, versus velocity magnitude, $V_0 := ||V||_0$), with validation sets in bold green. Different symbols and dashed lines show grouping into similar conditions, used to select suitably distributed validation sets and for preliminary evaluations. The grouping intervals were chosen so as to obtain similarly sized groups where possible.

Due to the manual trimming procedure and inevitable slight differences between separate flights, the exact same flight condition could not be replicated repeatedly. Rather, a grid of trim conditions was covered, as shown in Fig. 2. This can be seen as an advantage because the full domain can be covered more effectively, allowing for small differences to be considered. To facilitate some of the subsequent evaluations, the test manoeuvres were subdivided into five groups, as shown in Fig. 2. It can also be observed in the figure that the flight envelope does not uniformly cover the potentially achievable rectangular domain given by the upper and lower bounds of the velocity and AOA. Instead, only a limited area around a two-dimensional line is covered. This does not point to incompleteness of the flight data, rather, it suggests that there is some correlation between velocity and AOA, and that the inherently stable FWMAV is pulled towards an equilibrium condition. Therefore, the typical operating conditions of the test platform fall within this limited range. The coverage within the range considered is also not even; in particular, there is a more sparse region in the middle, which may have some effect on the results. Finally, it should be noted that the choice of variables to define the flight envelope is to some extent arbitrary, and it is indeed possible that additional parameters are necessary to fully describe the envelope, however the current selection was found to represent an effective starting point.

# III.  Flight envelope analysis and local modelling

Two steps were performed prior to developing global models, so as to glean information on the system behaviour and select a suitable global modelling approach. Firstly, the collected flight data were evaluated, and, secondly, local linearised models were identified. Both evaluations were focused on the flap cycle-averaged behaviour, under the assumption that the flapping component can be neglected due to time-scale separation, found in previous work to be acceptable for system-level dynamic analysis of this entomopter.[18] This assumption is also introduced to simplify the evaluation of the modelling approach – the inclusion of flapping effects will be considered in future work, if the approach is found to be promising. This section discusses the main findings of the aforementioned preliminary evaluations. The local models also constitute the basis of the global modelling process developed subsequently in this paper.

## III.A.  Local model estimation

While flapping-wing dynamics are highly complex, warranting investigation into multi-body modelling,[37,11,38,39] several studies have demonstrated that for basic considerations, e.g. in the context of design and control work, the conventional fixed-wing aircraft equations of motion represent a suitable description for many insects and FWMAVs.[5,40,41,18] Thus, local models were obtained using a simplified approach, shown in previous work to yield accurate local models for the studied test platform.[18]

To narrow down the global modelling problem, and given that the effect of the time-varying component on the body dynamics was found to be minor,[18] the time-varying component was neglected in this study. Furthermore, only the longitudinal dynamics were considered. Once a global modelling approach has been established for the time-averaged longitudinal component, the lateral dynamics and time-varying effects can be considered in future work.

The time-averaged longitudinal dynamics were assumed to have the following linear time-invariant (LTI) structure:[18]

$$
\begin{bmatrix} \Delta\dot{q} \\ \Delta\dot{u} \\ \Delta\dot{w} \\ \Delta\dot{\Theta} \end{bmatrix} = \begin{bmatrix} \frac{M_q}{I_{yy}} & \frac{M_u}{I_{yy}} & \frac{M_w}{I_{yy}} & 0 \\ \frac{X_q}{m} - w_0 & \frac{X_u}{m} & \frac{X_w}{m} & g\cos(\Theta_0) \\ \frac{Z_q}{m} + u_0 & \frac{Z_u}{m} & \frac{Z_w}{m} & g\sin(\Theta_0) \\ 1 & 0 & 0 & 0 \end{bmatrix} \begin{bmatrix} \Delta q \\ \Delta u \\ \Delta w \\ \Delta\Theta \end{bmatrix} + \begin{bmatrix} \frac{M_{\delta_e}}{I_{yy}} \\ \frac{X_{\delta_e}}{m} \\ \frac{Z_{\delta_e}}{m} \\ 0 \end{bmatrix} \Delta\delta_e
\tag{1}
$$

The above model structure is based on the nonlinear fixed-wing flight dynamics equations of motion, with minor differences in the linearisation process (e.g. accounting for the large pitch attitude in flight). An LTI model of the local longitudinal dynamics was identified from each of the 46 flight manoeuvres, resulting in 46 local models, covering a significant part of the achievable flight envelope (cf. Sec. II.C). For each dataset, the parameters in Eq. 1 were determined using a maximum likelihood estimator, as described in Ref. 18.

With the exception of one case (test # 9), where the estimation data were somewhat unsteady prior to the manoeuvre and adversely affected the result, all of the identified local models were found to be accurate for the corresponding conditions, as clear from the metrics in Table 2. As seen in the aforementioned table (cf. also Ref. 18), the accuracy is slightly lower for the velocities – especially for the $w$-velocity, for which the data appeared to be less informative. In general, the pitch dynamics are captured more accurately than the velocities, possibly because the elevator deflections used as input have a more significant effect on the former.

As stated in Sec. II.B, and as evident from Eq. 1, elevator signals were used to excite the system. Such signals were found in previous work to provide suitable excitation. A number of throttle manoeuvres (causing changes in flapping frequency) were collected in addition to the discussed data, in an attempt to better excite the velocity dynamics, in particular the component related to the force parallel to the fuselage ($Z$) – however, the overall excitation provided by throttle signals was found to be significantly more limited, and did not lead to a significant increase in excitation of the $Z$-force component, hence the decision to focus first on elevator manoeuvres. More complex types of input signals, e.g. based on some form of optimal input design,[42,43] may allow for improved excitation and hence improved results. Such signals will be considered in future work, and may allow for a more accurate representation of the velocity dynamics, however it is also possible that the velocity dynamics do not vary as significantly as the pitch dynamics or cannot be excited independently from the pitch dynamics, which would make this component difficult to model reliably.

**Table 2:** Metrics quantifying the performance of the local models (eq. 1); values show average±standard deviation over all datasets.

| Variable | Output corr. | RMSE (% of meas. range) |
|:---:|:---:|:---:|
| $q$ | $0.96 \pm 0.10$ | $4.2 \pm 3.0$ |
| $u$ | $0.94 \pm 0.10$ | $6.2 \pm 3.9$ |
| $w$ | $0.93 \pm 0.15$ | $6.8 \pm 5.3$ |
| $\Theta$ | $0.97 \pm 0.06$ | $3.9 \pm 2.6$ |

## III.B.   Data and local model analysis

Initially, the flight data were analysed to establish how and to what extent the system dynamics change in different flight conditions and hereby to help guide the modelling approach. Thus, for instance, an assessment was made of the change in measured responses to the same input signal in different flight conditions. Fig. 3(b) shows an example of this: here, the average responses of the manoeuvres conducted in each of the six groups of flight conditions (cf. Fig. 2), respectively, are shown together. This provides an idea of the trends in the output behaviour with the flight condition, and the magnitude of the changes. It can be seen that different trim conditions lead to visible differences in the resulting system response to the same input – in both magnitude, and especially phase. Moreover, these differences are small – they are likely to be significant, given the overall small scale considered, however they may be difficult to model accurately with real, noisy flight data. From flying experience with the studied ornithopter, it is known that there are noticeable differences in flight behaviour in the range of conditions considered. However, one additional goal of this study is to evaluate to what extent a global model is necessary in the considered range, and whether such small-scale differences can be modelled on the basis of real-world measurements.
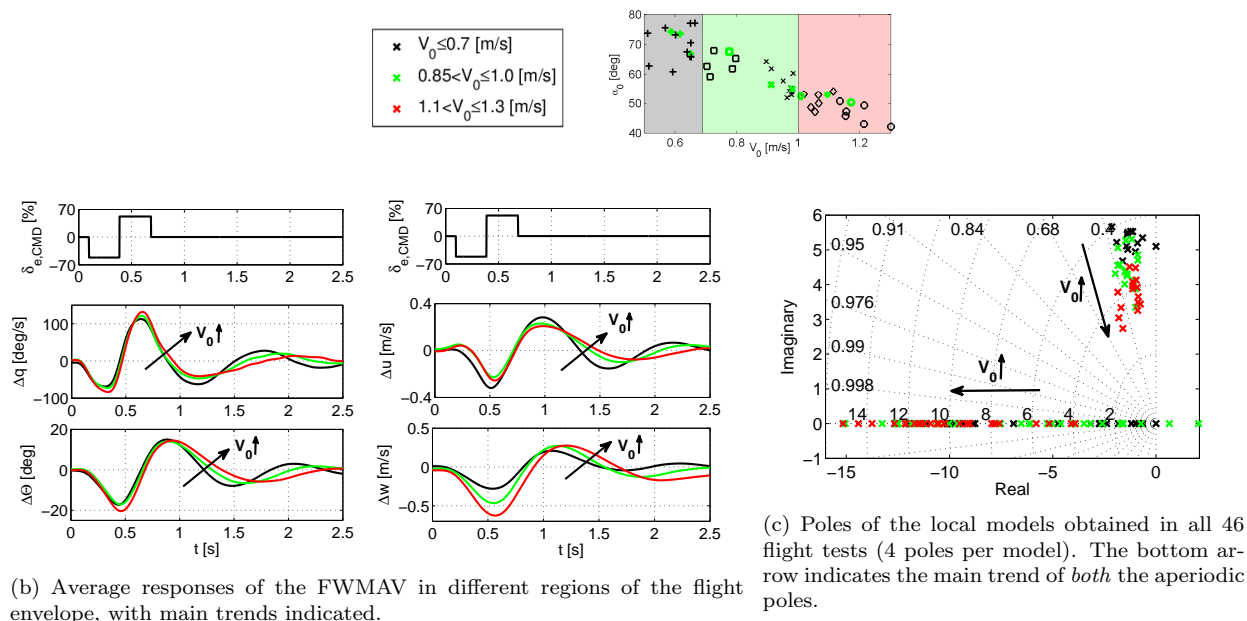


(b) Average responses of the FWMAV in different regions of the flight envelope, with main trends indicated.

(c) Poles of the local models obtained in all 46 flight tests (4 poles per model). The bottom arrow indicates the main trend of *both* the aperiodic poles.

**Figure 3:** Trends in system dynamics and output, with changing flight conditions.

Next, the obtained local linear models were considered. Such models constitute a helpful tool to analyse and quantify the changing dynamics of a system, which in turn is a useful starting point for global modelling. An analysis of the system dynamics was thus conducted as described in more detail in Ref. 34[a]. As anticipated from the data analysis, a number of clear trends were found in the system poles. As already observed in previous work,[36, 18] the FWMAV has one oscillatory pole and two aperiodic poles. In this case, all of the poles are stable except for two of the identified local models (cf. Fig. 3(c)). With increasing velocity (and

---

[a]Note that there are minor differences with the results in the reference as different flight test data are used here.

decreasing AOA), the oscillatory pole pair moves clearly towards lower frequencies. The damping appears to vary only to a minor extent and less clearly (cf. Sec. V.C for further discussion). The slower aperiodic pole varies from approximately -1 to -10 with increasing velocities, indicating a clear increase in stability. The faster pole, however, varies less consistently. It is interesting to note that for this particular eigenvalue, the current results do not fully agree with previous results obtained on the same vehicle,[34] suggesting that this component of the dynamics cannot be reliably captured and/or may be affected by parameters other than the velocity and AOA. One likely reason for the large variation and unclear trends is insufficiently informative data. Indeed, it was found that a number of parameters – especially those connected to the $w$-velocity – are estimated significantly less effectively, resulting in high variances, as discussed further in Sec. III.D. It is possible that better excitation of the corresponding dynamics can be obtained through different input sequences, but it is also possible that this part of the dynamics is generally less dominant compared to others, making it more challenging to excite and hence estimate. Some trends were also observed in the control behaviour, with the vehicle becoming more responsive to elevator deflections at higher velocities. As expected, this is mainly evident in the reaction of the pitch rate to the elevator, whilst the (indirect) effect on the velocities is both less significant overall, and less affected by the changing flight conditions (e.g., cf. Sec. III.D).

The system dynamics will be evaluated in more detail, in Sec. V.C, after the final model structure has been established. Nevertheless, the initial evaluation outlined in this section clearly suggests that changes in the dynamics are present within the operating domain considered, and already provides some information on the system dynamics and useful insight for global modelling. The main implications of the local modelling results for global modelling are summarised in the following section.

### III.C.    Main conclusions for global modelling

Based on the analysis in the previous sections, two main conclusions were drawn that are relevant for global modelling. Firstly, it was shown in Sec. III that LTI models of the suggested form (cf. Eq. 1) achieve a high accuracy at a local level, and can be used to describe the system dynamics in the entire region of the flight envelope analysed so far. This implies that the simplest possible approach to obtain global coverage is to somehow combine the available local models. This is also a highly advantageous approach from a control perspective, as a wide array of established control methods are available for LTI model structures. Secondly, within this region, there is a visible correlation between the local linear system dynamics and the flight conditions the respective local models refer to. Fig. 3 for instance highlights that with changing velocity (for example), the eigenvalues move in a clearly defined way within the complex plane, suggesting that at least some of the system properties change in different flight conditions. The aforementioned points suggest that linearised models provide a suitable local description, but also that the flight dynamics are in fact nonlinear, at least to some extent, even within the limited domain considered so far, and hence that global modelling is relevant. Moreover, based on these observations, a linear-parameter-varying (LPV) approach appears to be a suitable and indeed advantageous way to model the observed nonlinearity.

The preceding analysis also raised a number of questions to be considered in the global modelling process. One challenge is the fact that the observed differences between different local models are, in an absolute sense, small. Given that the considered scale is itself small – as is by definition the case for any MAV – even small differences in system behaviour may have a considerable impact, however, such differences are challenging to model accurately using flight data, which are inherently affected by noise and error. Another challenge is the fact that some components appear to be less reliably estimated than others, at the local level (cf. also Sec. III.D), which, clearly, will have adverse effects on the global modelling process. A similar problem may be posed by the somewhat unclear trends highlighted in some components of the dynamics: it is likely that these are mostly due to insufficient excitation, however it is also possible that the current definition of the flight envelope does not account for all the changes in the system behaviour. Alternative formulations, e.g. involving the flapping frequency, were considered but did not yield a significant improvement in the results, which, again, would seem to suggest that estimation issues are at the origin of the somewhat unclear variation in some components. The aforementioned factors may complicate the finding of an accurate global model of the system dynamics, although it is also possible that a global model will improve on the local results, by ignoring single outlier results in favour of the overall trends.

One possibility to address the challenge of unreliably-estimated components, without recurring to additional flight tests, is to adjust the local model structure and potentially exclude components that cannot be accurately determined, if these do not significantly affect the overall accuracy of the result. Thus, prior to

American Institute of Aeronautics and Astronautics

proceeding with the global modelling methodology, an assessment of the local model structure is made in the next section, with the object of improving the reliability and accuracy of the global modelling result.

## III.D.  Simplified local model

Despite the overall accurate local modelling results, a number of the local parameters were found to be unreliably estimated. Given that the LPV model will be constructed out of the local models, prior to proceeding to the global modelling, it is important to ensure that the local results are as accurate and reliable as possible, and to address known limitations where possible. In this context, the local model structure was revisited in an attempt to ensure a more accurate and more reliable final global model.

While the overall accuracy of the local models was found to be high, even for the less well-modelled components ($w$), it is possible that some of the parameters have no significant effect and therefore the parameter estimates themselves are essentially meaningless, which may influence the global model, as defined in this paper. Thus, an important question to consider, is whether the separate local model parameters are well-estimated and whether they are all necessary in the model structure.

The simplest evaluation that can be made, is to consider the estimated model parameters themselves, how they are distributed and how much and in what way they vary. Regarding the latter point, due to the different flight conditions covered, variation is expected, nonetheless, implausible and erratic variation can serve as a further indication that a particular parameter is not estimated reliably. When the accuracy and reliability of a local parameter is particularly low, for any of the reasons mentioned, the corresponding estimates may be meaningless. This is likely the case where the estimates for the same local parameter obtained from different datasets vary erratically and significantly, sometimes to an implausible extent. It can for instance be observed that the parameters $X_w$ and $Z_{\delta_e}$ vary significantly between different local models, not only in magnitude but also in sign. Given that the final state-output predicted by the local models was nonetheless accurate for all datasets, the significant variation implies that these parameters have no significant effect on the overall model (as determined from the current estimation data) and could be discarded from the local model structure with no significant effect. To a lesser extent, similar observations were made for all remaining $Z$-related parameters.

To evaluate the identifiability of single local model parameters, the estimated covariance matrices (Cramér-Rao bounds) of the original local models were considered next. Fig. 5 shows the estimated standard errors ($\hat{\sigma} := +\sqrt{var(\hat{\theta})}$) of the model parameters. The figure plots the distribution of the errors obtained for all local models, i.e. number of occurrences in each range of values. It can be observed that for some of the parameters, particularly those related to the $Z$-force and/or the $w$ velocity, the standard errors tend to be higher, with values frequently above 10% and reaching up to 50% in some cases. This implies that a lower confidence can be placed on the estimated parameter values, which points to a lower identifiability, and at least partially explains the seemingly more random variation of said parameters with the flight condition. For the remaining parameters, standard errors are mostly low for all datasets, typically below 5% and often much lower – suggesting that the local values are reliable.

Finally, it may be insightful to consider the estimated correlation coefficient between pairs of parameters in the local models. While the correlations between parameter pairs were rarely found to exceed the critical value of 0.9,[31] the values obtained nonetheless provide insight into which parameters have similar effects. The $w$ velocity-related parameters, for instance, were found to be generally more correlated to other parameters. Overall, with one exception, the correlations between parameters only exceeded the critical value in isolated cases, all of these occurring in the same two local model, which presumably were not effectively estimated as a whole. The exception is the parameter pair $[Z_q, Z_{\delta_e}]$: these two parameters were found to be almost fully correlated (corr>0.98) for a significant number of the local models, suggesting that for one of the reasons discussed in Sec. III.B they cannot be estimated separately with any reliability, and hence it is advisable to drop one of the two from the model structure.

Based on the preceding discussion, a more reliable and accurate modelling result may be obtainable by fixing the less reliably estimated local parameters to zero a priori, i.e. excluding them from the local model structure, so that the main effects can be better captured by the remaining parameters, which in turn may facilitate the construction of an accurate global model. Specifically, the following parameters were discarded: $X_w, Z_u, Z_{\delta_e}$. Note that the decision to discard $Z_u$ rather than $Z_w$ was to some extent arbitrary, as both parameters appeared to be unreliable to a similar extent. $Z_q$ was retained because it was found to affect the result, despite not being estimated clearly – this parameter will be re-evaluated in Sec. V.B.
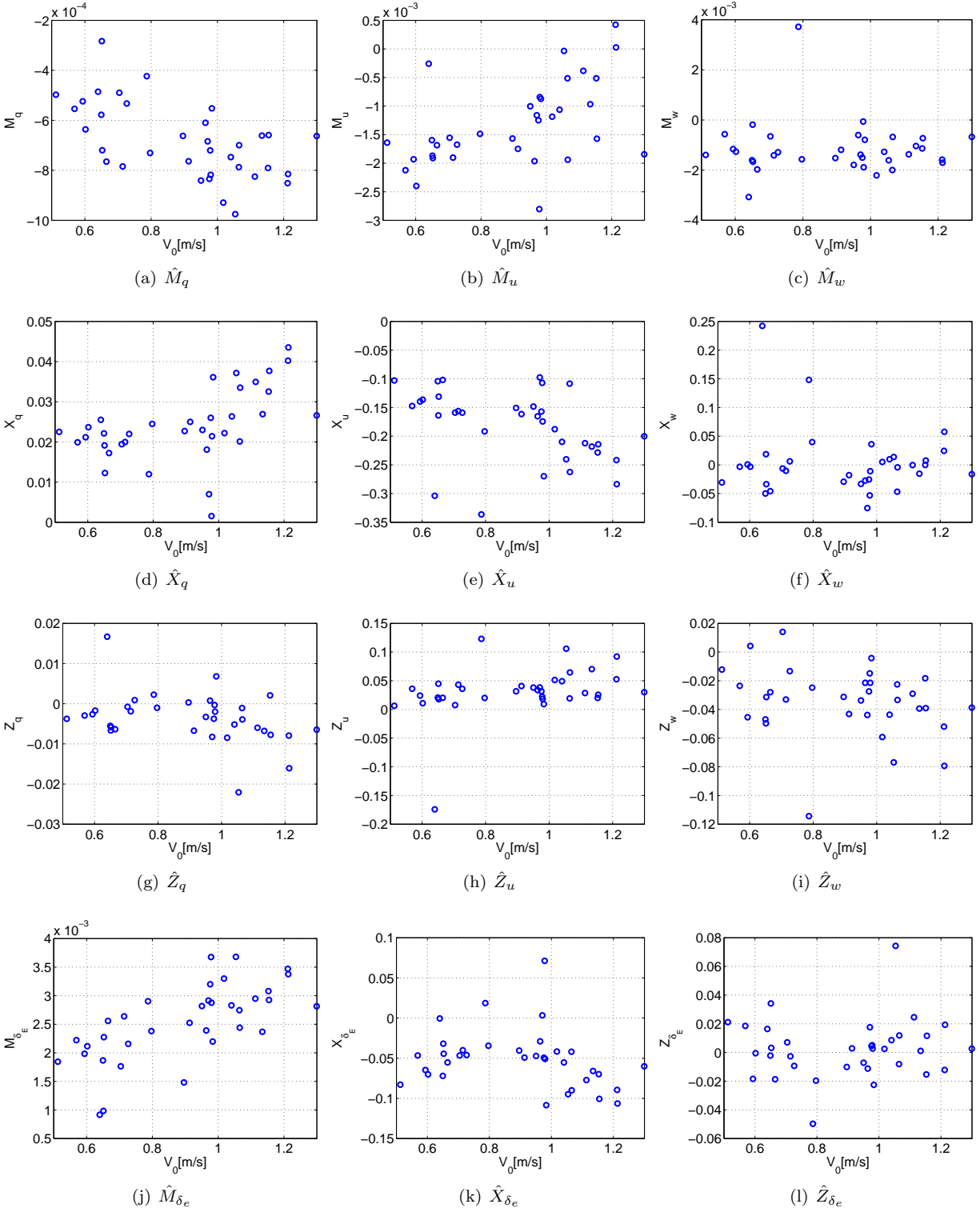
**Figure 4:** Local LTI model parameters versus flight velocity (cf. Fig. 2).

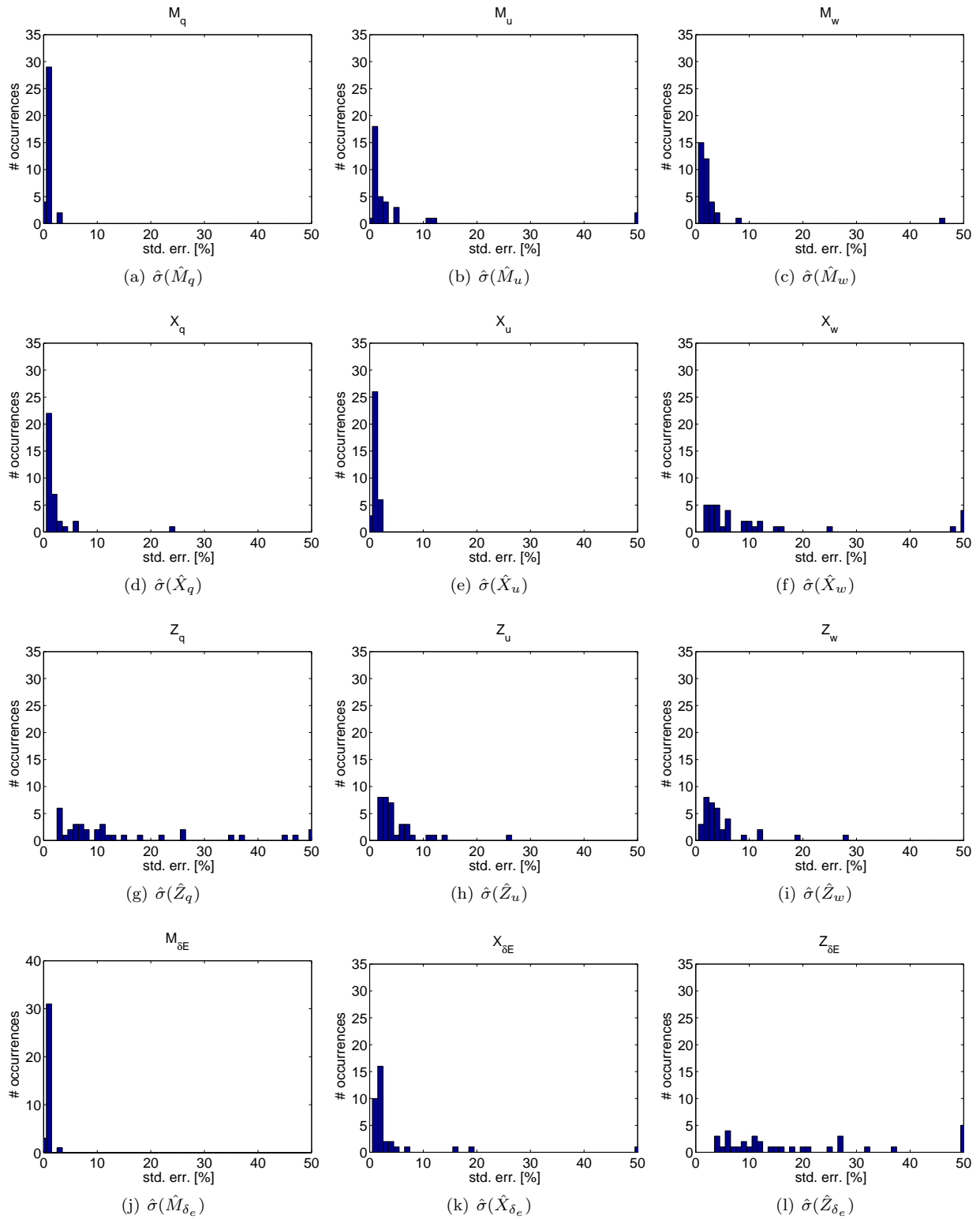**Figure 5:** Estimated standard errors for each local LTI parameter estimate, using the **full model structure (Eq. 1).**
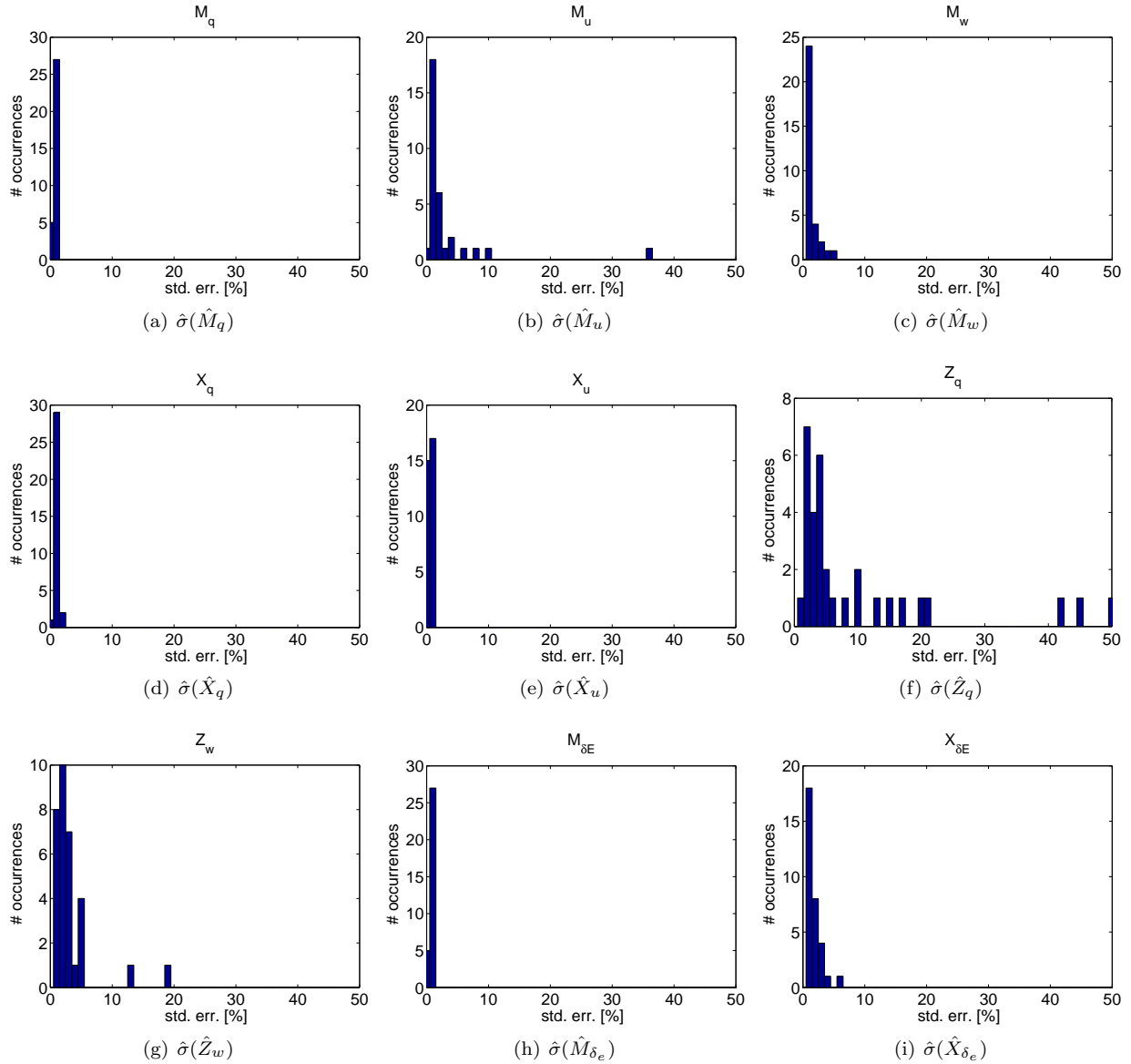
**Figure 6:** Estimated standard errors for each local LTI parameter estimate, using the **simplified model structure** (Eq. 2).

The resulting simplified model structure was thus the following:

$$
\begin{bmatrix} \Delta \dot{q} \\ \Delta \dot{u} \\ \Delta \dot{w} \\ \Delta \dot{\Theta} \end{bmatrix} = \begin{bmatrix} \frac{M_q}{I_{yy}} & \frac{M_u}{I_{yy}} & \frac{M_w}{I_{yy}} & 0 \\ \frac{X_q}{m} - w_0 & \frac{X_u}{m} & 0 & g\cos(\Theta_0) \\ \frac{Z_q}{m} + u_0 & 0 & \frac{Z_w}{m} & g\sin(\Theta_0) \\ 1 & 0 & 0 & 0 \end{bmatrix} \begin{bmatrix} \Delta q \\ \Delta u \\ \Delta w \\ \Delta \Theta \end{bmatrix} + \begin{bmatrix} \frac{M_{\delta_e}}{I_{yy}} \\ \frac{X_{\delta_e}}{m} \\ 0 \\ 0 \end{bmatrix} \Delta \delta_e \tag{2}
$$

Results were found to be slightly better than for the original model, both in terms of output accuracy (cf. Table 3) and in terms of consistency and reliability, while requiring a smaller number of parameters. While the $Z$-equation parameters are still less accurately estimated than the rest, there is an improvement in the parameter covariances (cf. Fig. 6) even in these parameters. The remaining parameters are all estimated reliably and, as will be discussed subsequently in Sec. V.B, they display clearer trends with the flight conditions, where such trends appear to be present. The previously identified problem of highly correlated parameters was also no longer found to be present.

**Table 3:** Metrics quantifying the performance of the simplified local models (eq. 2); values show average±standard deviation over all datasets.

| Variable | Output corr. | RMSE (% of meas. range) |
|:---:|:---:|:---:|
| $q$ | $0.97 \pm 0.02$ | $4.0 \pm 1.2$ |
| $u$ | $0.96 \pm 0.02$ | $5.7 \pm 1.9$ |
| $w$ | $0.94 \pm 0.07$ | $6.9 \pm 3.2$ |
| $\theta$ | $0.98 \pm 0.02$ | $3.9 \pm 1.2$ |

# IV.  Global modelling

## IV.A.  LPV approach

Linear parameter-varying (LPV) modelling is closely related to the idea of gain scheduling in control.[44,45] The underlying concept is that at every point in the operating domain of a system a linearised model can be obtained, and that a function can be found to interpolate between these linearised models, based on some arbitrary scheduling variable. As a result, the same model structure can be used to describe the entire operating domain, in dependence on a set of scheduling variables. Ideally, the scheduling variables should be exogenous and independent of the system dynamics.[46,47] In this sense, LPV methods are best suited to systems with clearly defined, discrete operating conditions, where independent external scheduling variables can be easily defined. Nonetheless, the LPV approach has been applied to systems that do not strictly meet this requirement, including aircraft.[23,24,25,48,26] Many aircraft applications in fact use a so-called quasi-LPV approach, where the scheduling variables are (or depend on) system states but are assumed to be independent. Furthermore, many aerospace examples of LPV modelling linearise an available nonlinear model to obtain a linearised model structure that contains the chosen scheduling variables.[25,30] The aim is frequently to simplify the nonlinear model to allow for simpler control approaches to be applied.

In the current study, no baseline model is available, thus it is not possible to derive from first principles an LPV model structure, where the scheduling variables can be defined somewhat intuitively and related to physical parameters. Instead, the choice of scheduling variables and scheduling functions is to some degree arbitrary, as discussed subsequently. The LPV model was implemented by scheduling the individual model parameters, i.e. the state-space matrices in Eq. 1, as described in Sec. IV.B. Note that while the term scheduling is adopted to describe the functions used to approximate the changes between local models, the resulting global model will not be identical to the local models at the flight conditions the latter are estimated in. In fact, given that the baseline local models are themselves not ideal, *true* descriptions of the system, and that the observed variation in local dynamics may not depend exclusively on the chosen scheduling variables, it was considered inadvisable to interpolate between the local models. Doing so would result in highly complex functions, both counteracting the object of simplified modelling, and almost inevitably producing a global model that captures the error as well as the system dynamics. Instead, it was considered preferable to find a function that approximates the most significant trends observed in a somehow optimal

way. The chosen approach is based on the assumption that the parameters are sufficiently uncorrelated to each other (cf. also Sec. III.D) and that the model structure remains the same for all conditions considered. Both assumptions are already made, implicitly, in the local modelling process, and, while both are not wholly valid, the obtained local results suggest that they are acceptable. The following sections outline the LPV modelling approach formulated within this study. An in-depth treatment of the general LPV modelling framework can be found in the literature (e.g.,[20,47,46]).

## IV.B.   Scheduling formulation

As for the previously discussed local modelling, the first step in the global model identification process is to define a suitable model structure. For LPV modelling, this involves defining both a local model structure and a set of scheduling functions to combine the local models. In view of the already available local models, the structure of the LPV model was based on that of the local LTI models (cf. Eq. 1), however in the LPV model each parameter is a function of some of the states rather than a constant, i.e.:

$$\dot{\mathbf{x}} = \mathbf{A}(\rho)\mathbf{x} + \mathbf{B}(\rho)\mathbf{u} \tag{3}$$

where $\rho$ is the vector of scheduling variables and the system matrices $\mathbf{A}$ and $\mathbf{B}$ are no longer constant but depend on $\rho$. Assuming the dependence on the scheduling variables is affine, this can be written out as:

$$\mathbf{A}(\rho) = \mathbf{A}_0 + \mathbf{A}_1\rho(1) + \mathbf{A}_2\rho(2) + \ldots + \mathbf{A}_n\rho(n) \tag{4}$$
$$\mathbf{B}(\rho) = \mathbf{B}_0 + \mathbf{B}_1\rho(1) + \mathbf{B}_2\rho(2) + \ldots + \mathbf{B}_n\rho(n) \tag{5}$$

where the bracketed number denotes the corresponding component in the scheduling vector $\rho$, and the matrices $\mathbf{A}_i$ and $\mathbf{B}_i$ are matrices of coefficients for the $i$th of the $n$ elements in the scheduling vector. Note that the matrices on the right hand side do not have to be full, and in the current problem are indeed mostly sparse (cf. Eq. 16).

Once the underlying local model structure has been defined, the key question in devising an LPV model structure is the selection of suitable scheduling variables. In conventional fixed-wing problems, LPV models are typically scheduled based on either flight states, or configuration-related variables.[24,23,29,30] Based on the analysis in Sec. III.B and on previous work,[36,34] and given that a single configuration (i.e. CG and geometry) was considered, functions of the (trim) angle of attack (AOA), total velocity and flapping frequency were considered as a basis for scheduling in the current model. Given that accurate results were found to be obtainable using only the AOA and velocity (excluding the flapping frequency), however, the remainder of this paper focuses on these two variables only. Moving from the general notation in Eqs. 4–5 to the specific formulation used in this study, the scheduling vector $\rho$ thus takes the form:

$$\rho_{ij}(V_0, \alpha_0) := V_0^i \alpha_0^j, \quad i \in [0, d], j \in [0, d], \tag{6}$$

where $d$ is the maximum degree considered for each scheduling variable. It should be noted that the entire set of possible combinations obtainable from Eq. 6 was merely the starting point for model structure selection, whereas the final model structure includes only a small number of these terms (cf. Sec. IV.C).

Given that certain components of the local model structure are known and entirely determined by kinematic relations, the scheduling was limited to the aerodynamic terms, while the known parts of the local model structure were kept at their known values, or determined from known expressions, as clarified in Eq. 7. In some cases it may be more convenient, in practice, to directly interpolate the entire matrices – if this is the case, it is straightforward to adjust the current model formulation to also include the kinematic terms, particularly since all of these terms are either constant or known to be related to the chosen scheduling states. The resulting LPV model, as formulated in the current study, takes the following form, where tilde

superscripts denote parameters estimated from the scheduling functions.

$$
\tilde{\mathbf{A}}(V_0, \alpha_0) = \begin{bmatrix} \frac{\tilde{M}_q}{I_{yy}} & \frac{\tilde{M}_u}{I_{yy}} & \frac{\tilde{M}_w}{I_{yy}} & 0 \\ \frac{\tilde{X}_q}{m} - w_0 & \frac{\tilde{X}_u}{m} & \frac{\tilde{X}_w}{m} & g\cos(\Theta_0) \\ \frac{\tilde{Z}_q}{m} + u_0 & \frac{\tilde{Z}_u}{m} & \frac{\tilde{Z}_w}{m} & g\sin(\Theta_0) \\ 1 & 0 & 0 & 0 \end{bmatrix}
$$

$$
:= \begin{bmatrix} 0 & 0 & 0 & 0 \\ -w_0 & 0 & 0 & g\cos(\Theta_0) \\ u_0 & 0 & 0 & g\sin(\Theta_0) \\ 1 & 0 & 0 & 0 \end{bmatrix} + \sum_{i=0}^{d} \sum_{j=0}^{d} \mathbf{A}_{ij}\rho_{ij}(V_0, \alpha_0) \tag{7}
$$

$$
\tilde{\mathbf{B}}(V_0, \alpha_0) = \begin{bmatrix} \frac{\tilde{M}_{\delta_e}}{I_{yy}} \\ \frac{\tilde{X}_{\delta_e}}{m} \\ \frac{\tilde{Z}_{\delta_e}}{m} \\ 0 \end{bmatrix} := \sum_{i=0}^{d} \sum_{j=0}^{d} \mathbf{B}_{ij}\rho_{ij}(V_0, \alpha_0) \tag{8}
$$

As in Eqs. 4 and 5, $\mathbf{A}_{ij}$ and $\mathbf{B}_{ij}$ are constant matrices of coefficients[b], however, here their subscripts indicate which component of the scheduling vector they refer to. Given that not all permutations given by Eq. 6 are used in the final model structure, and that finally different parameters will be represented by different scheduling functions, several $\mathbf{A}_{ij}$ and $\mathbf{B}_{ij}$ matrices in the above equations will be either zero or sparse matrices. As a further clarification, the LPV component of Eqs. 7 and 8 can be written out for each parameter in the model structure ($\mathbf{A}$ and $\mathbf{B}$ matrices) as shown below for, e.g., $\tilde{M}_q$:

$$
\tilde{M}_q(V_0, \alpha_0) = \sum_{i=0}^{d} \sum_{j=0}^{d} a_{Mq,ij}\rho_{ij} = a_{Mq,00} + a_{Mq,01}\rho_{01} + \ldots + a_{Mq,dd}\rho_{dd} \tag{9}
$$

Here $a_{Mq,ij}$ denotes the set of constant global model parameters (contained in the $A_{ij}$ matrices in Eq. 7) that are used to compute $\tilde{M}_q$ at any given flight condition, given the velocity and AOA. Note that in the analogous of the above equation written for parameters in the *local* $\mathbf{B}$ matrix, the *global* model parameters are denoted by a $b$ instead of an $a$ (e.g. $b_{M\delta_e,ij}$). The different notation is merely used to highlight the relation between the scheduling functions and the local model structure at the basis of the global model.

The derivation of the scheduling functions, and estimation of the global model parameters they contain $(A_{ij}, B_{ij})$, are explained in the following section.

## IV.C. Scheduling function selection and global model parameter estimation

Clearly, Eqs. 4 and 5 result in a large number of terms even if a small polynomial degree $d$ is chosen for the scheduling functions. In fact, only a small number of terms were found to be required on the right hand side of the equations, resulting in a relatively simple final result. To determine which of the potential terms are necessary for accurate global modelling, and to determine suitable functions to describe each term in the LPV model, a stepwise regression was implemented, starting from a candidate pool of model terms including all parameters shown in the above equation, up to a degree of $d = 3$ for each model term. The maximum model degree was limited to avoid excessively high orders that might have led to over-fitting. Additionally, lower-order functions are more likely to retain a basic level of physical plausibility.

Given that considering the LPV model output (i.e. the model-predicted states) directly in the stepwise regression would have required optimising the model structure for all scheduling functions simultaneously, as well as for all flight conditions simultaneously, resulting in a computationally expensive problem, the problem was simplified by assuming that all local model parameters are entirely uncorrelated (cf. Sec. IV.A). This was considered an acceptable assumption based on the relatively low correlations obtained between separate parameters in the local models (cf. Sec. III.D), and allows for each term in the LPV model to be considered separately. It was thus assumed that finding the optimal model structure for each sub-model would lead to a suitable global model structure, albeit not an optimal one.

---

[b]$\mathbf{A}_{ij}$ and $\mathbf{B}_{ij}$ contain the *global* model parameters, which are constant for all flight conditions

A stepwise regression was thus conducted for each parameter in the $\mathbf{A}_{ij}$ and $\mathbf{B}_{ij}$ matrices ($\tilde{M}_q$, $\tilde{M}_u$, etc.), in order to determine a scheduling polynomial to represent the parameter as a function of the scheduling variables $(V, \alpha)$. This was attempted both with the AOA and velocity alone, and with the two aforementioned variables together with the flapping frequency. Initial results demonstrated that a high accuracy can be achieved even if the flapping frequency is excluded – a solution considered preferable as it results in a simpler model structure.

Details on stepwise regression can be found in the literature (e.g., Refs. 49, 31, 50); a concise overview is given here for completeness. Stepwise regression is a model structure determination process for problems that can be expressed as a linear regression, in the form:

$$\mathbf{z} = \mathbf{X}\boldsymbol{\Theta} + \epsilon \tag{10}$$

where $\boldsymbol{\Theta}$ is a constant parameter vector, $\epsilon$ is the equation error, and $\mathbf{z}$ and $\mathbf{X}$ contain the output and regressors, respectively, at each measurement point.

Based on the previously stated assumption that the local model parameters are uncorrelated, each parameter in the local model structure was treated separately. Thus, for each local parameter ($M_q$, $M_u$, etc.), the above equation is constructed as follows: the parameter vector contains the global model parameters (e.g. the $a$ terms in Eq. 9) used to represent the *local* model parameter considered; the output vector contains the values the considered local parameter takes in each of the identified local models ($\mathbf{z} \in \mathbb{R}^{n_C \times 1}$, where $n_C$ is the number of flight conditions considered); and the regressor matrix contains functions of $V$ and $\alpha$ computed from measurements at every flight condition, starting from all $n_x$ combinations given by Eq. 6 ($\mathbf{X} \in \mathbb{R}^{n_C \times n_x}$). Each measurement instance (row of $\mathbf{z}$, $\mathbf{X}$ and $\epsilon$) therefore corresponds to a different flight condition.

Thus, for instance, for $M_q$, Eq. 10 takes the form,

$$
\begin{bmatrix}
M_q(V(1), \alpha(1)) \\
M_q(V(2), \alpha(2)) \\
\vdots \\
M_q(V(n_C), \alpha(n_C))
\end{bmatrix}
=
$$

$$
\begin{bmatrix}
\rho_{00}(1)=1 & \rho_{01}(1)=\alpha(1) & \cdots & \rho_{dd}(1)=V^d(1)\alpha^d(1) \\
\rho_{00}(2)=1 & \rho_{01}(2)=\alpha(2) & \cdots & \rho_{dd}(2)=V^d(2)\alpha^d(2) \\
\vdots & \vdots & \ddots & \vdots \\
\rho_{00}(n_C)=1 & \rho_{01}(n_C)=\alpha(n_C) & \cdots & \rho_{dd}(n_C)=V^d(n_C)\alpha^d(n_C)
\end{bmatrix}
\begin{bmatrix}
a_{Mq,00} \\
a_{Mq,01} \\
\vdots \\
a_{Mq,dd}
\end{bmatrix}
+
\begin{bmatrix}
\epsilon(1) \\
\epsilon(2) \\
\vdots \\
\epsilon(n_C)
\end{bmatrix}
\tag{11}
$$

The main limitation of the model formulation in Eq. 10 is that it cannot account for the error in the velocity and AOA measurements, and only considers the error $\epsilon$ in the local model parameters, assumed, as per convention, to be white Gaussian noise. Nonetheless, the aforementioned model formulation provides a straightforward means to derive suitable scheduling functions, and was subsequently found to yield accurate final results (cf. Sec. V).

Given an equation of the form of Eq. 10, the goal of the stepwise regression process is to determine which of the $n_x$ regressors in $\mathbf{X}$ need to be retained in order to obtain an accurate model. The stepwise regression thus begins from a pool of candidate regressors, constructed out of permutations of the velocity and AOA, up to the chosen maximum model degree (here, 3; cf. also Eqs. 6 and 9). At each step, the partial correlation of each regressor with the known output $z$ is computed, accounting for any already determined model terms (i.e. we compute the correlation of the regressor to the original output $z$ minus the contribution of the model terms included in previous steps). The regressor $x_k$ leading to the highest partial correlation is considered for inclusion in the model structure, and the (partial) F-statistic is calculated[50] to determine whether the contribution of the selected regressor to the model is significant, i.e. whether F is above a chosen critical value:

$$F_k = \frac{\hat{\theta}_k^2}{\sigma^2(\hat{\theta}_k)} > F_{crit} \tag{12}$$

where $\hat{\theta}_k$ is the considered parameter (which is multiplied by regressor $x_k$ in the model), and $\sigma^2$ is the estimated variance of $\theta_k$. If Eq. 12 holds, then the corresponding parameter $\hat{\theta}_k$ is included in the model. Whenever a new model term has been added, the partial F-statistic of all regressors previously included in the model structure must be re-computed, to assess whether their contribution remains significant after

the additional variable has been included in the model structure. Any of the previously included regressors whose F-statistic is below the chosen threshold is once again removed from the model. These steps are repeated until some criterion is met; in this case, the change in predicted square error and $R^2$ coefficient were considered.

Once a model structure has been selected, the global model parameters are estimated using an ordinary least squares (OLS) estimator, which lends itself well to the model formulation used in the regression. Using the same notation as in Eq. 10, the cost function to minimise, for each local parameter ('output' $\mathbf{z}$), is given by:

$$\mathbf{J} = \frac{1}{2} \left[\mathbf{z} - \mathbf{X\Theta}\right]^T \left[\mathbf{z} - \mathbf{X\Theta}\right]^T \tag{13}$$

where $X^*$ denotes the final, optimised set of regressors resulting from the stepwise regression. The OLS estimator resulting from the minimisation process is then:

$$\hat{\mathbf{\Theta}} = (\mathbf{X}^T\mathbf{X})^{-1}\mathbf{X}^T\mathbf{z} \tag{14}$$

The set of global model parameter vectors $\hat{\mathbf{\Theta}}$ (one per local model term) allows for an LTI model to be obtained in any part of the known flight envelope and, theoretically, also to extrapolate beyond this. The latter however requires further investigation of the boundaries of the flyable envelope and of the nonlinearity of the system outside the explored region. The high-level process to determine the scheduling functions and global model parameters is clarified in Fig. 7
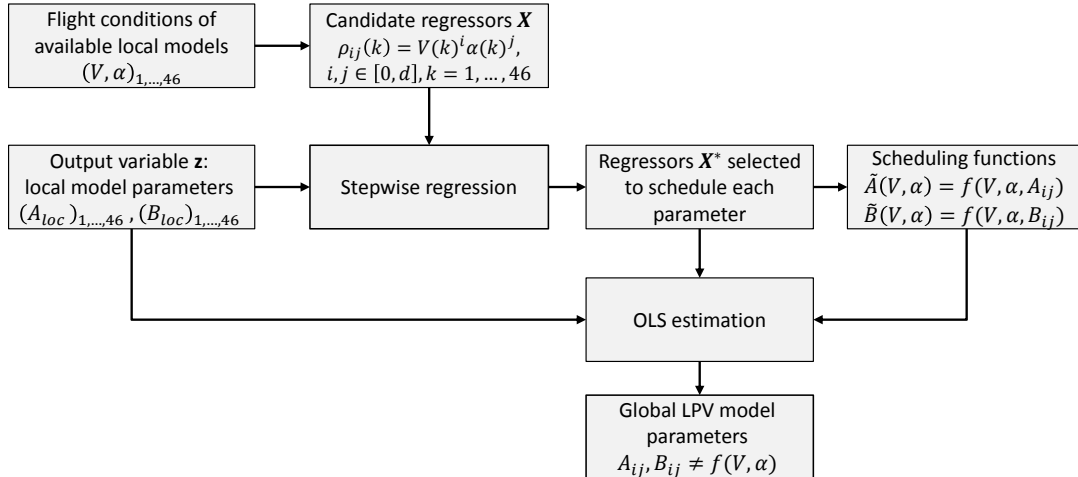


**Figure 7:** Diagram schematically illustrating the LPV model construction process. $\mathbf{X}^*$ represents the final regressor matrix obtained after the stepwise regression process.

## IV.D.    Average model for comparison

The alternative to expressing each model parameter as a function of the flight condition, is to use a constant value. In order to provide a worst-case comparison for the developed LPV model, we also defined an *average* model, with a single set of parameters, which we applied to the entire flight envelope considered, to establish whether and to what extent global modelling is necessary for the considered test platform. To account for the fact that the flight test data are not distributed in a uniform manner, the average model was obtained by calculating a weighted average for each parameter in the local model structure from the parameter values of all the local models. In particular, each model parameter was weighted with its distance from the calculated geometric centre $(\bar{V}, \bar{\alpha})$ of the considered flight envelope, defined as the difference between maximum and minimum V and AOA, respectively, for each of the two spatial coordinates. Each parameter in the average

model was thus defined as,

$$\theta_{avg} := \begin{cases} \frac{\sum \theta_k(V_k,\alpha_k)r_k}{\sum r_k} & \text{if} \quad r_k \neq 0 \forall k \\ \theta(\bar{V},\bar{\alpha}) & \text{if} \quad \exists r_k(r_k = 0) \end{cases} \quad , \qquad r_k := \sqrt{(V_k - \bar{V})^2 + (\alpha_k - \bar{\alpha})^2} \qquad (15)$$

where $\theta$ represents any parameter in the **A** and **B** matrices defining the model structure (i.e. $M_q, M_u$, etc.). The second clause of the equation is included to account for the possibility of local models identified at the defined centre of the flight envelope. As no such models were available, effectively only the first clause of the equations was used. To ensure a fair comparison also in the validation phase, only the estimation datasets were used to compute the average model.

As clear from Eqs. 7 and 8, a distinction is made between the aerodynamic and purely kinematic components of the LPV model. This may be inconvenient for some applications, but it is trivial to extend the modelling approach to also include the kinematic terms, while the current formulation allows for additional insight into the flight properties of the studied platform to be obtained. Thus, in an analogous way, two different average models were considered. The first average model is an overall weighted average, defined directly by Eq. 15. Here also the kinematics-related terms are averaged. The second average model involves averaging only the aerodynamic components according to Eq. 15, while the kinematic terms are assumed to be known at any flight condition. The latter model hence can be seen as a partial average – i.e. an average of the aerodynamics only. In the majority of the evaluations that follow, the partial average model is used for comparison (henceforth, this model is termed 'average', while, where mentioned, the overall average model is denoted as 'full average'). This choice was made in order to differentiate between the effects of the aerodynamics and the kinematics, thus obtaining an idea of how the aerodynamics change. The results obtained with an overall average were found to be somewhat less accurate than those obtained with a partial average, but mostly in the same order of magnitude. In this sense, comparing the LPV model to the partial average can also be considered a conservative evaluation of how useful the global model is.

## V. LPV modelling results

### V.A. Preliminaries

This section presents the obtained global LPV model. Following an assessment of the scheduling results, the final LPV model is evaluated and compared to (i) the original local models, in the conditions where such models were available, (ii) the flight data collected in the same conditions, and (iii) the 'partial' average model presented in Sec. IV.D. Comparison to the local models represents the most basic form of evaluation, as the LPV model is based directly on the local models, and not on the flight data. Hence, this determined how accurate the LPV model is at reproducing the changing dynamics given by the local models. Comparison to flight data provides additional insight, given that while in theory the best possible outcome is for the LPV model to replicate the local models in the considered local conditions, in reality it is possible that the LPV model approximates the flight data better than the local models, as it does not represent a direct interpolation and may therefore compensate for irregularities in single local models/datasets. Finally, comparing to the average model was intended to evaluate to what extent a global model is necessary, and whether the suggested approach improves upon the worst-case option of using the same model throughout the flight envelope. Fig. 8 clarifies the relations between the three types of models.

Similarly, for the evaluations that follow, it is important to distinguish between (a) global model parameters, (b) estimated local model parameters, and (c) LPV model-estimated local parameters. The LPV model contains a set of global parameters (a), which are the same in all flight conditions. The LPV model can be used to estimate local parameters (b, henceforth 'LPV-estimated local parameters'): these are the values taken by the left hand side variables in Eqs. 7 and 8 (and all equations analogous to Eq. 9) if AOA and velocity values for a particular flight condition are substituted into the right hand side of the equations. The set of resulting calculated parameters yields an LTI model at the flight condition considered and can therefore be compared to the original estimated local model parameters (c) directly estimated in the same flight condition.

A number of flight test datasets were excluded from the model identification process and used only in the validation phase in order to assess the accuracy of the obtained model. For this, nine datasets were selected at random, distributed uniformly among the groups of datasets shown in Fig. 2, in relation to the group size. Several different random selections were investigated, and the comparable results obtained suggest a
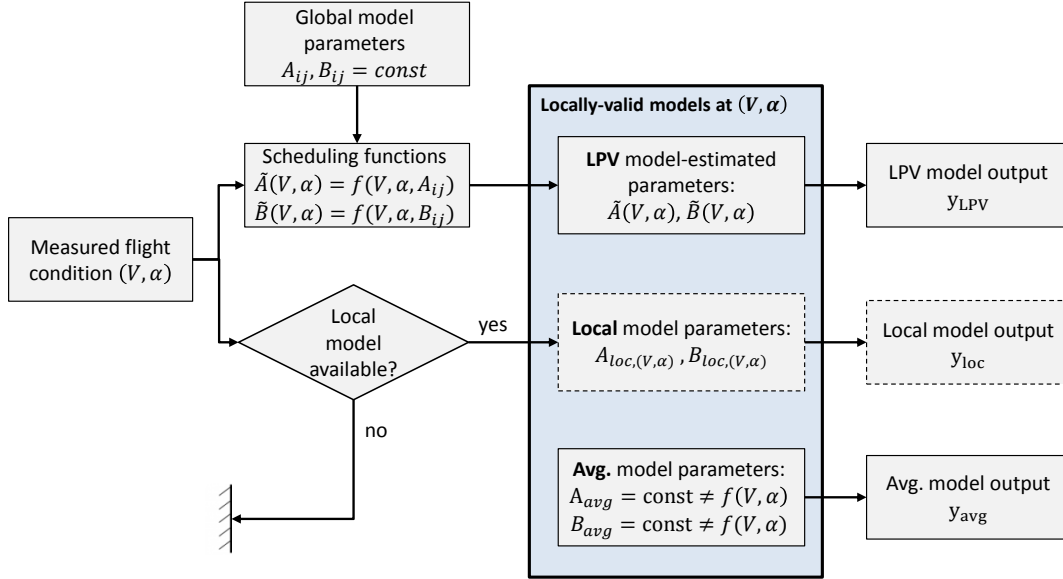
**Figure 8:** Diagram schematically illustrating the relationship between the global LPV model, and the set of local models and single average model that it is compared to.

degree of robustness of the modelling approach. In the remainder of this paper, results are shown for one of the estimation-validation selections (validation datasets: 3, 6, 11, 16, 22, 31, 32, 41, 45; shown in bold font in Fig. 2).

## V.B.   Scheduling results

Prior to considering the complete LPV model, it is useful to consider the (estimated) local model parameters in comparison to the corresponding parameters predicted by the LPV model in the same flight conditions (LPV model-estimated local parameters). This gives a preliminary indication of the accuracy of the resulting model and also provides further insight into the adequacy of the chosen model structure. Shortcomings in the LPV model are likely to be related to one of the following causes: (i) the parameter is not estimated accurately in the local models, (ii) the chosen LPV scheduling variables are unsuited to represent the variation of the particular local parameter considered, or (iii) the local parameter is generally unaffected by the flight condition. The first point may be due to insufficient excitation in the estimation data used, or because the parameter has a limited influence on the system dynamics (i.e. is superfluous to the model), or because it is strongly correlated to other parameters and therefore cannot be identified independently from these – these points were addressed in Sec. III.D. The second point is not considered at this stage, as the local analysis in Sec. III suggests that the velocity and AOA are suitable at least to capture the most significant trends in the dynamics. The third point is discussed in this section, in the context of the scheduling results. Based on this evaluation, final minor adjustments are made to the model structure, and the final LPV model is obtained, which is then discussed in depth in Sec. V.

The approach outlined in Sec. IV was applied, starting from the flight data presented in Sec. II.C and the local model structure defined in Sec. III.D, to obtain an LPV model covering the portion of the flight envelope explored in the current flight tests (cf. Fig. 2). Starting from the simplified local model structure defined in Eq. 2, the following scheduling functions were obtained from the stepwise regression process, conducted according to Sec. IV.C:

American Institute of Aeronautics and Astronautics

$$\tilde{M}_q = a_{Mq,00} + a_{Mq,10}V + a_{Mq,30}V^3$$
$$\tilde{M}_u = a_{Mu,00} + a_{Mu,10}V + a_{Mu,20}V^2 + a_{Mu,30}V^3$$
$$\tilde{M}_w = a_{Mw,00} := \bar{M}_w$$
$$\tilde{M}_{\delta_e} = b_{M\delta_e,00} + b_{M\delta_e,20}V^2 + b_{M\delta_e,21}V^2\alpha + b_{M\delta_e,30}V^3$$
$$\tilde{X}_q = a_{Xq,00} + a_{Xq,21}V^2\alpha$$
$$\tilde{X}_u = a_{Xu,00} + a_{Xu,11}V\alpha + a_{Xu,21}V^2\alpha \qquad (16)$$
$$\tilde{X}_w = 0$$
$$\tilde{X}_{\delta_e} = b_{X\delta_e,00} + b_{10}V + b_{X\delta_e,30}V^3$$
$$\tilde{Z}_q = a_{Zq,00} := \bar{Z}_q$$
$$\tilde{Z}_u = 0$$
$$\tilde{Z}_w = a_{Xw,00} + a_{Xw,01}\alpha + a_{Xw,11}V\alpha + a_{Xw,12}V\alpha^2$$
$$\tilde{Z}_{\delta_e} = 0$$

The bracketed expressions in the set of equations above denote parameters which were not scheduled in the final model. In fact, next to ensuring a suitable identifiability of the local model parameters at the basis of the chosen modelling approach (cf. Sec. III.D), the resulting LPV model can be further improved by determining whether the local parameters are in fact significantly related to the flight conditions and only scheduling the parameters that meet this requirement. While it was mentioned in Sec. III that the dynamics of the local models are related to the flight condition, this does not necessarily imply that each of the local parameters is correlated to the flight condition. Some parameters were found to be important for the system dynamics overall, but not to be significantly affected by different flight regimes, as defined in this paper and within the range considered, or to be difficult to predict accurately with simple functions of the AOA and velocity. While scheduling expressions for these parameters were still obtained from the stepwise regression, owing to the liberally chosen stopping criteria, the scheduling results suggested that not scheduling these parameters might have no significant effect on the result, as discussed further below.

The scheduling results obtained are shown in Fig. 9, which shows the local model parameters, the LPV model-estimated parameters for the same flight conditions, and the average model parameters (based on Sec. IV.D). While several parameters are dependent on a function of both the velocity and the AOA, the parameters are plotted against each of these two variables separately, to provide a clearer overview. Overall, it can be observed that most of the LPV model-calculated parameters take on values that are close to those of the local models in the corresponding conditions. Where there is a trend with the flight condition, the sub-models are capable of reproducing it accurately, as, for instance, clearly seen for $M_u, M_{\delta_e}, X_q$ and $X_u$. The parameters connected to the $Z$ force and $w$ velocity are less accurately predicted by the global model – these parameters were already estimated less reliably in the local models, it is therefore unsurprising that the global modelling result is equally inaccurate. It is also clear that while some parameters display a clear correlation with the flight condition, others display no clear trends even though they are estimated effectively in the local models. This suggests that it is unnecessary to enforce on all local parameters a correlation to the flight condition, and that a similar or better result may be obtainable by keeping some parameters fixed to constant values (e.g. the value from the average model in Eq. 15) and only varying the remaining parameters. This would allow for simpler models that still capture the main effects. Based on a visual evaluation, local model parameters that do not appear to vary with the flight regime include $M_w$ and $Z_q$.

A quantitative evaluation of the accuracy of the chosen LPV model – and, to some extent, the degree of correlation of local parameters and flight conditions – can also be obtained by computing, for each parameter, the correlation between local parameter estimates obtained in all flight conditions and corresponding LPV model-predicted parameters. Additionally, probability values (p-values) can be considered to evaluate the significance of said correlations. Based on these metrics, shown in Table 4, it can be observed that most of the parameters retained in the simplified local model structure are modelled effectively by the chosen LPV formulation, with the exception of $M_w$ and $Z_q$, which do not display significant trends with the flight condition, and hence are not accurately predicted by the chosen LPV scheduling functions. The parameters $X_\delta$ and $Z_w$ are also significantly less correlated to the flight conditions compared to the remaining parameters, however the obtained results suggest they may still be possible to model.
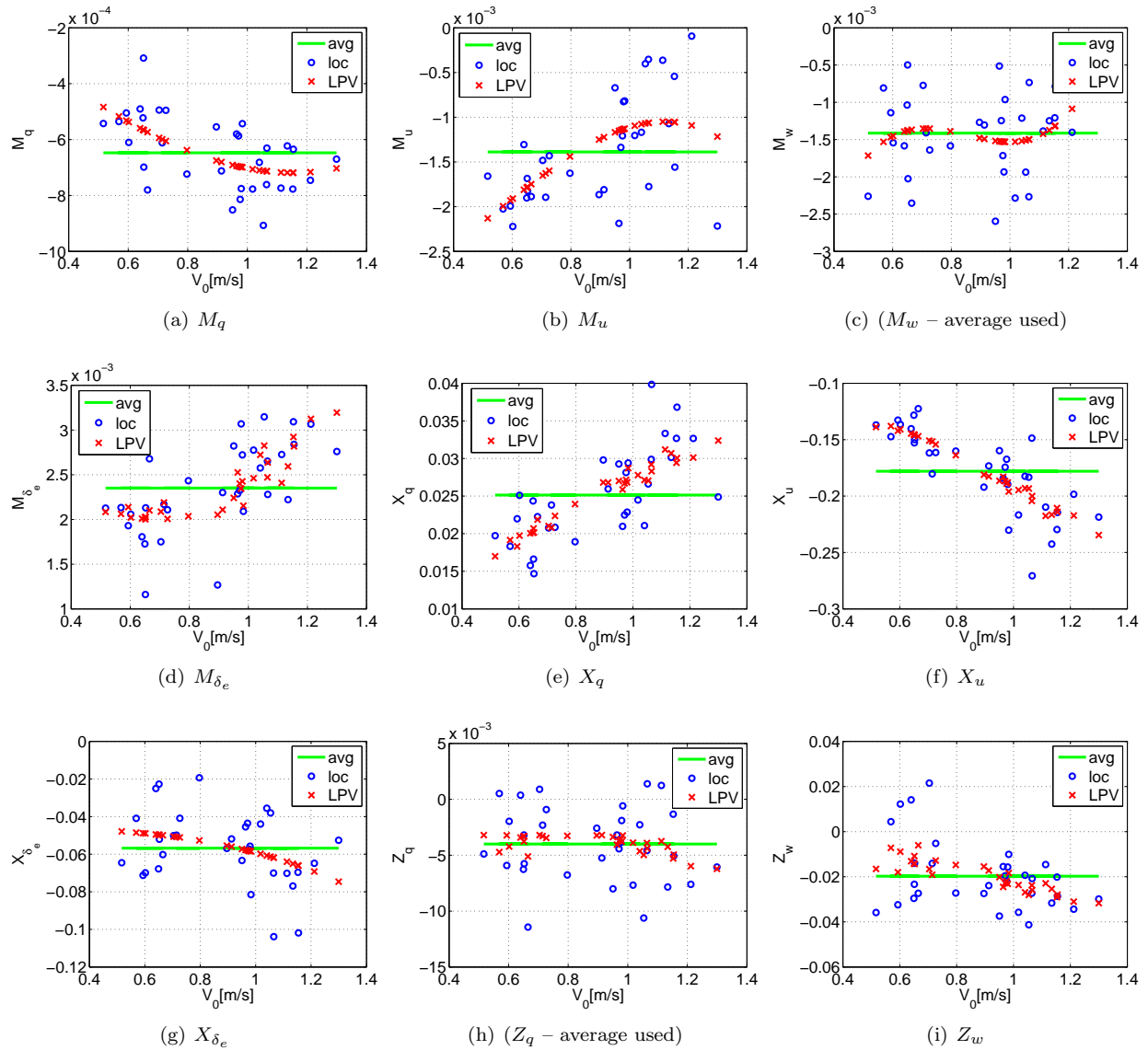
**Figure 9:** Estimated LPV parameters compared to corresponding LTI model parameters, in flight conditions where local models are available. Local LTI model parameters, and corresponding parameters estimated from the LPV model, plotted versus the trim flight velocity (cf. Fig. 2). The average of each parameter over all 46 LTI models is also shown for comparison.
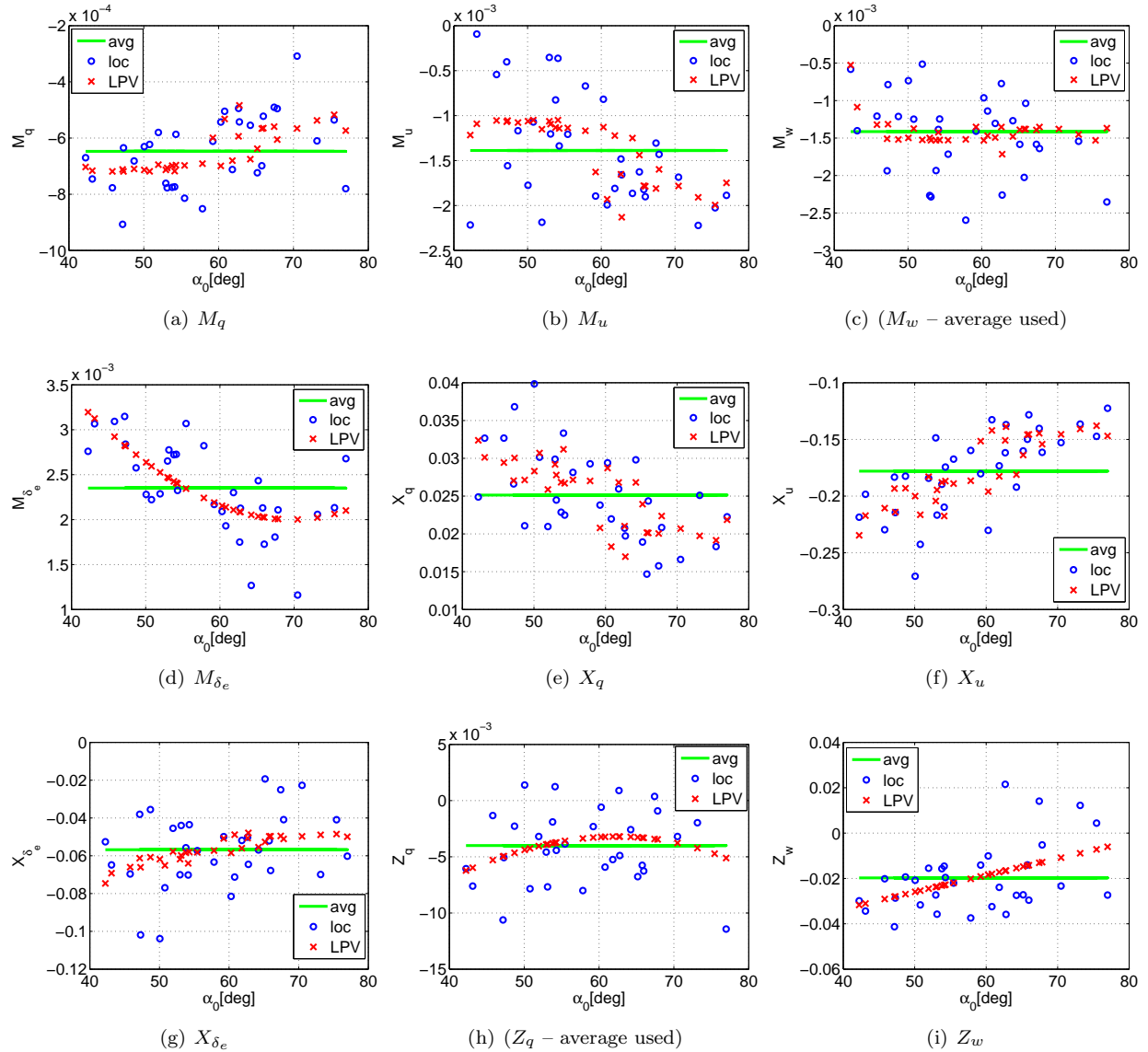
**Figure 10:** Estimated LPV parameters compared to corresponding LTI model parameters, in flight conditions where local models are available. Local LTI model parameters, and corresponding parameters estimated from the LPV model, plotted versus the trim angle of attack (cf. Fig. 2). The average of each parameter over all 46 LTI models is also shown for comparison.

**Table 4:** Full model structure: correlation between LPV-estimated parameters and local model values; and corresponding p-values (statistical significance).

| Param. | $\mathbf{corr}(\tilde{\theta}_{\mathbf{LPV}}, \hat{\theta}_{\mathbf{loc}})$ | p-value |
|:------:|:------:|:------:|
| $M_q$ | 0.61 | $\ll 0.001$ |
| $M_u$ | 0.75 | $\ll 0.001$ |
| $M_w$ | 0.22 | 0.23 |
| $M_{\delta_e}$ | 0.71 | $\ll 0.001$ |
| $X_q$ | 0.78 | $\ll 0.001$ |
| $X_u$ | 0.83 | $\ll 0.001$ |
| $X_{\delta_e}$ | 0.52 | 0.003 |
| $Z_q$ | 0.06 | 0.73 |
| $Z_w$ | 0.55 | 0.002 |

Based on all the preceding considerations, the parameters $M_w$ and $Z_q$ were fixed to average values (obtained from the average model in Eq. 15. The following LPV model structure was thus chosen for the final, simplified (subscript 'simp') global model:

$$\tilde{\mathbf{A}}_{\mathbf{simp}}(V,\alpha) = \begin{bmatrix} \frac{\tilde{M}_q(V)}{I_{yy}} & \frac{\tilde{M}_u(V)}{I_{yy}} & \frac{\bar{M}_w}{I_{yy}} & 0 \\ \frac{\tilde{X}_q(V,\alpha)}{m} - w_0 & \frac{\tilde{X}_u(V,\alpha)}{m} & 0 & g\cos(\Theta_0) \\ \frac{\bar{Z}_q}{m} + u_0 & 0 & \frac{\tilde{Z}_w(V,\alpha)}{m} & g\sin(\Theta_0) \\ 1 & 0 & 0 & 0 \end{bmatrix}, \tag{17}$$

$$\tilde{\mathbf{B}}_{\mathbf{simp}}(V,\alpha) = \begin{bmatrix} \frac{\tilde{M}_{\delta_e}(V,\alpha)}{I_{yy}} \\ \frac{\tilde{X}_{\delta_e}(V)}{m} \\ 0 \\ 0 \end{bmatrix} \tag{18}$$

where a bar superscript indicates that the corresponding parameter is fixed to the same constant value (viz. a weighted average obtained from all estimation datasets) regardless of the flight condition, rather than being computed from the scheduling functions. Note that the parameters in Eq. 18 are now estimated from the *global* model, as denoted by the tilde superscript, and can therefore be calculated in any flight condition. The scheduling functions used to obtain the unknown parameters in the above expression were given previously in Eq. 16. Substituting the estimated global model parameters into the aforementioned equation gives the following final scheduling functions:

$$\begin{aligned}
\tilde{M}_q &= -7.45 \times 10^{-3} - 3.49 \times 10^{-2} V + 7.11 \times 10^{-3} V^3 \\
\tilde{M}_u &= -4.21 \times 10^{-2} - 1.80 \times 10^{-1} V + 1.64 \times 10^{-1} V^2 \\
\tilde{M}_w &= -7.21 \times 10^{-2} \\
\tilde{M}_{\delta_e} &= 8.26 \times 10^{-2} + 2.04 \times 10^{-1} V^2 - 0.10 \times 10^{-1} V^2 \alpha - 6.25 \times 10^{-2} V^3 \\
\tilde{X}_q &= 1.24 \times 10^{-2} + 1.60 \times 10^{-2} V^2 \alpha \\
\tilde{X}_u &= -1.39 \times 10^{-1} + 8.25 \times 10^{-2} V\alpha - 1.37 \times 10^{-1} V^2 \alpha \\
\tilde{X}_w &= 0 \\
\tilde{X}_{\delta_e} &= -1.29 \times 10^{-1} + 1.56 \times 10^{-1} V - 8.10 \times 10^{-2} V^3 \\
\tilde{Z}_q &= -4.15 \times 10^{-3} \\
\tilde{Z}_u &= 0 \\
\tilde{Z}_w &= -3.87 \times 10^{-1} + 3.46 \times 10^{-1} \alpha + 3.67 \times 10^{-1} V\alpha - 3.48 \times 10^{-1} V\alpha^2 \\
\tilde{Z}_{\delta_e} &= 0
\end{aligned} \tag{19}$$

American Institute of Aeronautics and Astronautics

Results were also computed using the original full local model (Eq. 1) with no further adjustments. The simplified model structure was found to yield somewhat improved results, while requiring only approximately half the number of parameters, therefore it represents an attractive solution. Additionally, the new model structure improves on the original in terms of reliability of the results, by only including well-estimated parameters and only scheduling those parameters that vary significantly with the flight condition.

Ultimately, rather than by its parameters, a model must be judged by its dynamic properties and the output it predicts. These points are discussed in the next subsections.

## V.C.  System dynamics

The resulting model was first evaluated in terms of the system dynamics. This evaluation also provided more detailed insight into the dynamics of the test vehicle, which are therefore discussed again in this section. Note that the local modelling results shown in the remainder of this paper refer to the simplified model given by Eq. 2.

As discussed, the local LTI systems all have one complex pole pair and two real poles. Fig. 11 shows the full polar plots obtained from the LPV model in the 46 different flight conditions considered, the corresponding 46 local models, and the average model (cf. Sec. IV.D). The poles obtained from each model are also shown separately in Fig. 12, with colours illustrating the changes with changing flight velocity. Finally, to facilitate the evaluation of each component of the dynamics, the poles of each of the aforementioned models (or set of models) are plotted separately in Fig. 13, against the flight conditions the LPV model was evaluated at (corresponding to the conditions where local models were available). In the interest of clarity, the complex pole is split into real and imaginary components. Results obtained from the validation data are highlighted in the plots. Note that in this section – and in the figures shown – the flight condition is shown only in terms of the velocity. For the sake of clarity, it was decided to only evaluate one variable at a time. The velocity was chosen as it is the variable most correlated to most of the model parameters, however trends with the AOA were in most cases approximately inversely correlated and are therefore not shown.
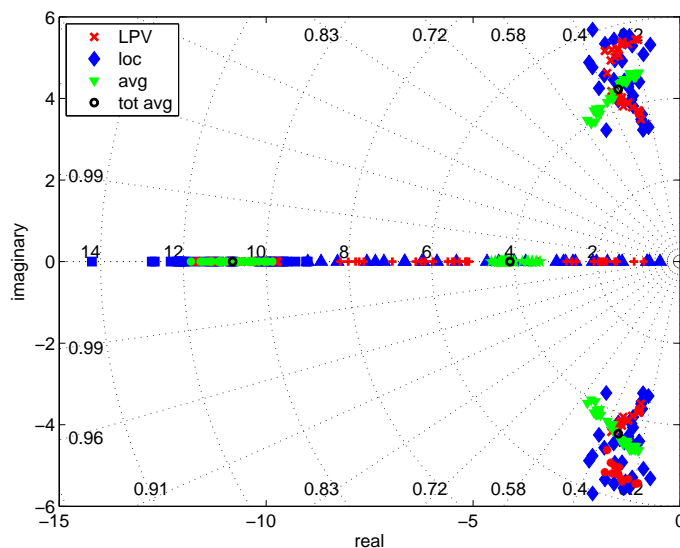


**Figure 11:** System poles in the complex plane: LPV, local and average models; overall average (with fixed kinematics) is also shown.

As already suggested in Sec. III.B, there are trends between the system poles and the flight conditions, however this is not the case, to the same extent, for all of the poles. The LPV model was found to replicate most of the observed trends, albeit some more accurately than others. As expected, the trends that emerged more clearly from the local modelling are replicated more accurately by the LPV model, while unclear variations in the local modelling results led to unclear global modelling results. This points to shortcomings in the underlying local models rather than in the global model.

The complex pole displays a clear trend with the flight condition, as evident from the trends highlighted in Figs. 13(b) and 13(a), and the analogous trajectory shown in Fig. 12. The imaginary component in particular, clearly decreases in magnitude at higher velocities - indicating that the frequency decreases.
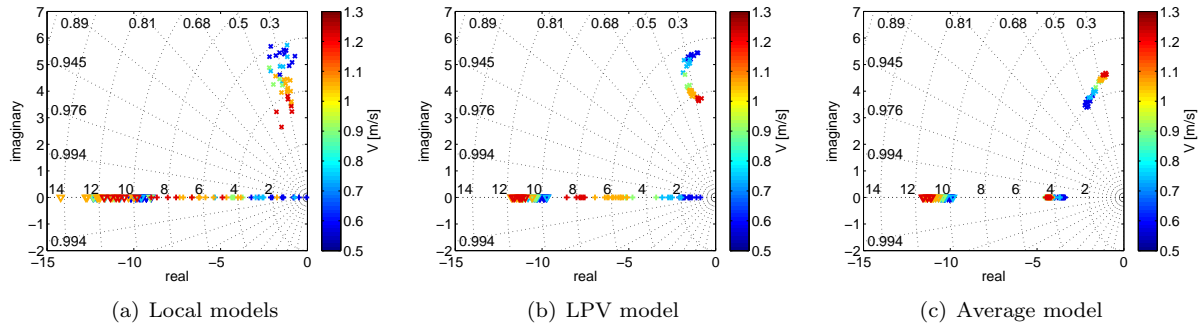
(a) Local models     (b) LPV model     (c) Average model

**Figure 12:** System poles in the complex plane: LPV, local and average models; with colour indicating changing flight velocity.



(a) $Re(p_1) = Re(p_2)$     (b) $Im(p_1) = -Im(p_2)$
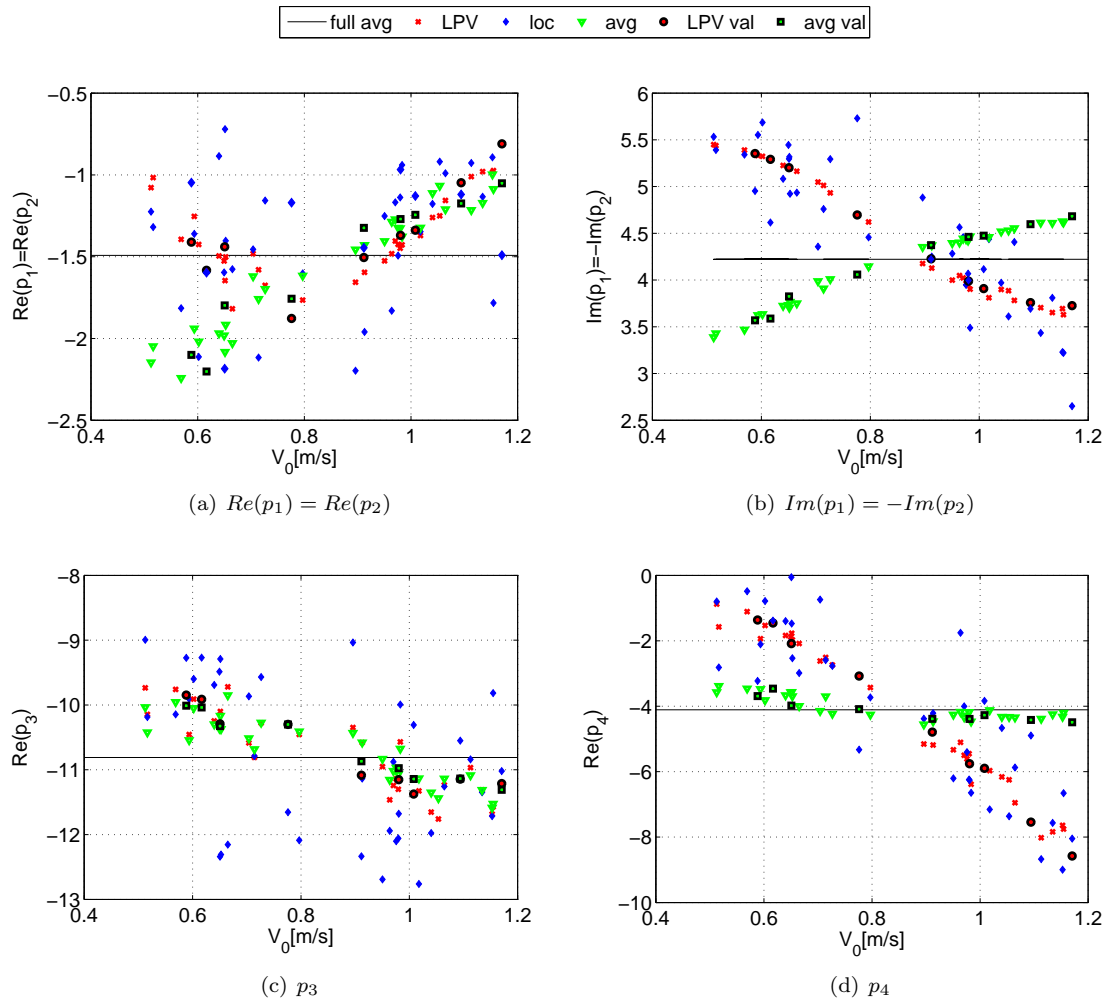
(c) $p_3$     (d) $p_4$

**Figure 13:** System poles versus corresponding trim velocity: LPV, local and average models (val=validation).

This trend is accurately captured by the LPV model. Interestingly, the average model, which considers the changing kinematics but not the changing aerodynamics, shows an opposite trend in the imaginary component, suggesting that the trend seen in the local model oscillatory dynamics (particularly in the frequency) is predominantly determined by the aerodynamics rather than by the kinematics. By contrast, the real component of the complex pole displays a considerably smaller overall variation and the local model-obtained values are more scattered, so that the variation with the velocity is less clear, particularly in the

American Institute of Aeronautics and Astronautics

low velocity range. Nonetheless, there appears to be a trend, which is captured by the LPV model, with the damping initially increasing, in the lower velocity range (up to $V \approx 0.8 m/s$), and then clearly decreasing again at even higher velocities. The average model that only considers kinematic changes, displays a very similar result in the high velocity range, but the trend does not reverse at low velocities, suggesting that at low velocities the aerodynamics play a more dominant role in determining the overall dynamic behaviour, compared to the (body) kinematics. It would also appear that there is a 'sweet spot' for the studied platform, where the damping is highest – and this is in agreement with piloting experience on the vehicle. However, the significant amount of seemingly random variation in the local data implies that these results must be verified and are not yet conclusive.

The faster of the two real poles ($p_3$) shows only a vague trend, decreasing somewhat at higher velocities, however there is a large amount of variation between the local model results, and further (and ideally better) data would be required to ascertain this trend. Given the large amount of variation, while the LPV model captures a part of the trend, the result is not clear, especially in the higher velocity range. Here, the LPV and average models are almost identical – this may be because of the parameters that were fixed to constant values or excluded from the model structure, which imply that parts of the LPV model-predicted dynamics (i.e. the parts associated with the $Z$-force) will be very close to those predicted by the average model. Despite the somewhat unclear result, it should be noted that since this is the fastest pole, it should play only a limited part in the overall response. The slower pole ($p_4$) again displays a very clear trend with the flight condition, which is captured with significant accuracy by the LPV model. The average model, by contrast, barely captures any of this trend, and closely resembles the overall average, suggesting that this component of the dynamics too is determined by the aerodynamics rather than the kinematics. It can also be observed that, based on the observed trends, this pole appears to be become unstable at very low velocities and clearly unstable at hover. For a symmetrical tailless flapper at hover, $p_4$ captures the vertical dynamics.

Overall, the damping decreases at very low velocities. At higher velocities, the real poles become more negative but the oscillatory pole appears to eventually become unstable. The oscillatory component decreases in frequency at high velocities – in agreement with observed flight behaviour of the test platform. The significant differences between the local (and LPV model) trends and those shown by the kinematic model highlight that the aerodynamics are indeed changing with changing flight conditions, and suggest that the overall flight behaviour resulting is predominantly influenced by the aerodynamics, as opposed to the kinematics. Overall the LPV model is accurate in capturing those trends that are clearly visible and can be used to predict the changing dynamic properties of the system in different conditions, which may itself already be useful. However, it should be considered that additional effects may become evident with more informative data, in particularly data where the linear velocity dynamics are excited more effectively. The current result is mainly focused on the pitch dynamics, which for instance do not appear to have a significant effect on the fast aperiodic pole ($p_3$).

### V.D.    Output match

Figs. 14 and 15 show examples of the output predicted by the LPV model, compared to the flight data, the output of the corresponding local LTI models, and the output of the average model (where only the kinematics vary, cf. Sec. IV.D). Examples of results are shown for both the estimation and the validation datasets, with the specific datasets selected from different parts of the flight envelope so as to present a basic overview. A more comprehensive overview is given in Figs. 16–18, which show statistical metrics (RMS errors and output correlation coefficients) evaluating the performance of the LPV model for all estimation and validation datasets. Figs. 16 and 18, in particular, show the difference in performance, respectively, between LPV and average models, and between LPV and local models, facilitating the comparison of the different types of models. The same information is also summarised in Table 5.

As anticipated from the scheduling results (cf. Sec. V.B), it can be observed that the LPV model is able to approximate the local models, and hence the flight data, reaching a high level of accuracy for both the estimation and the validation conditions. The validation results, in particular, suggest that the model can be used to predict the flight behaviour at points where no local models are available. While the local models are consistently more accurate compared to the LPV results computed in the same conditions – as expected, given that the local models are the baseline used to construct the LPV model, and considered to be correct a priori – the differences between the set of local models and the LPV model are typically small. Generally, where the local models used for estimation have a somewhat lower accuracy, the LPV model also tends to perform less effectively, emphasising that an identified model can only be as good as the identification data

(a) Test #2 (low velocity/ high AOA condition)

(b) Test #14 (intermediate velocity/ AOA condition)

(c) Test #26 (intermediate velocity/ AOA condition)

(d) Test #38 (high velocity/ low AOA condition)
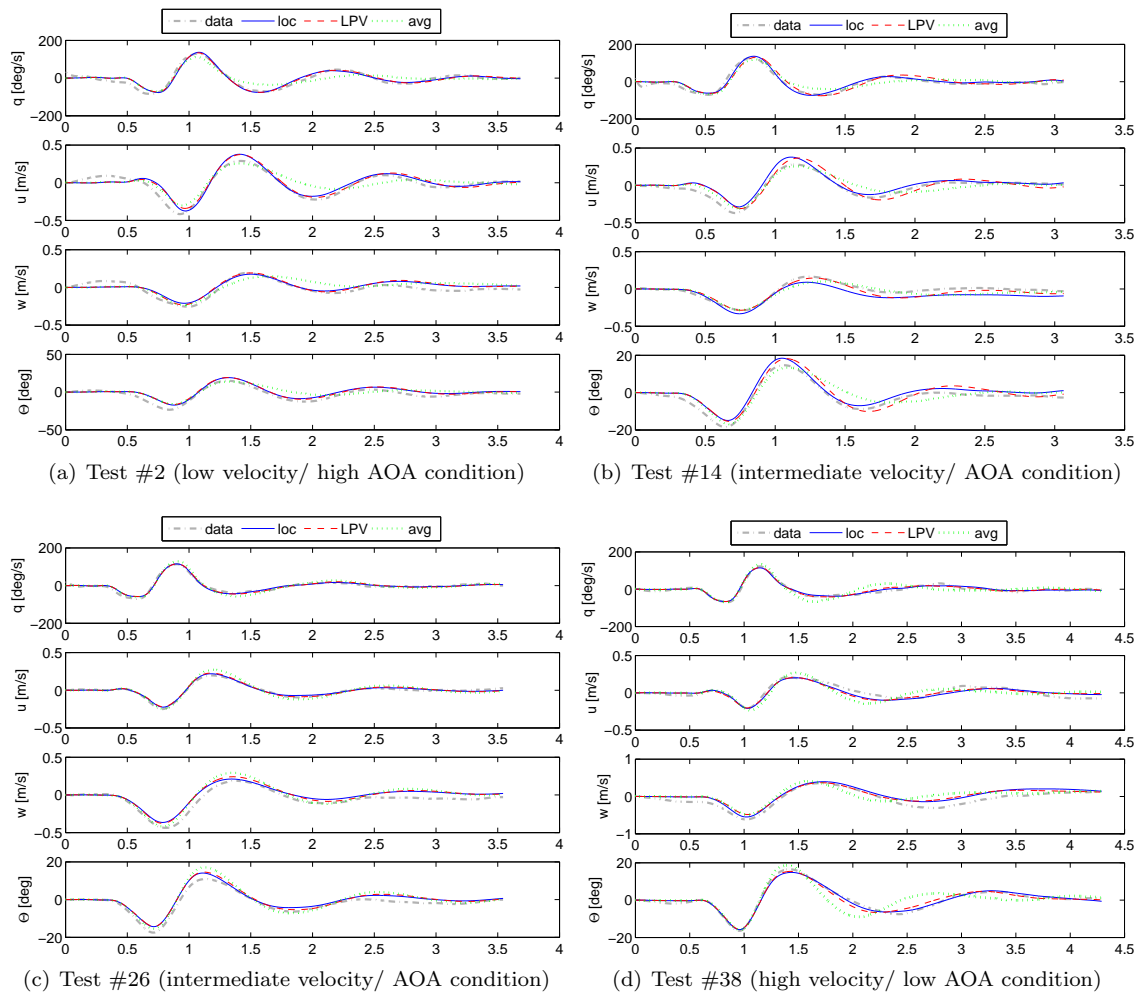
**Figure 14:** Example of output match: LPV, average and local models, versus flight test data (estimation sets)

(a) Test #3 (low velocity/ high AOA condition)

(b) Test #11 (intermediate velocity/ AOA condition)

(c) Test #22 (intermediate velocity/ AOA condition)

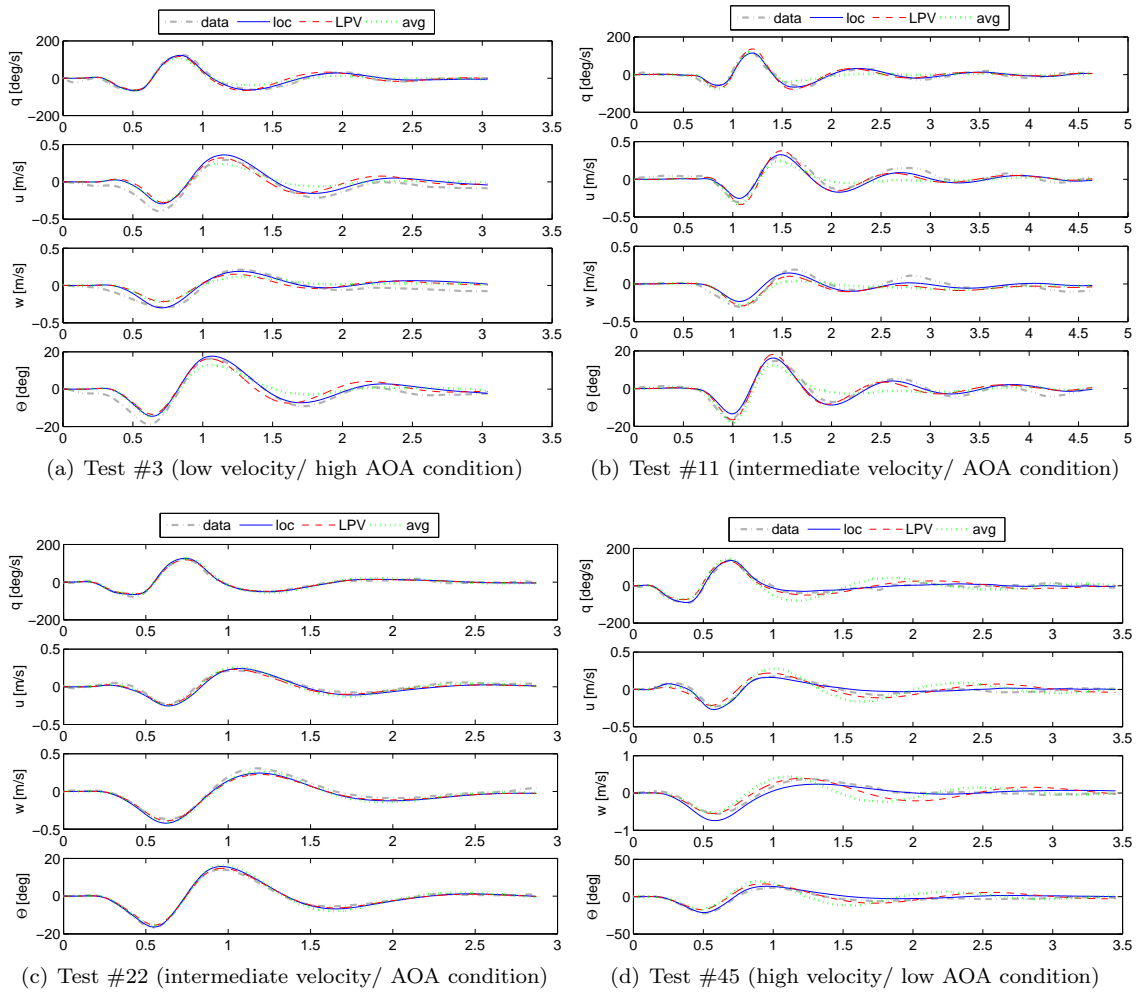(d) Test #45 (high velocity/ low AOA condition)

**Figure 15:** Example of output: reduced-order LPV, average and local models, versus flight test data (validation sets)

it is derived from. Nevertheless, amongst the flight conditions considered, there are isolated cases where the LPV model displays a marginally better performance than the corresponding local model (cf. Fig. 18) – these are cases where the relevant local model is comparatively less accurate, e.g. due to less clean or informative identification data, suggesting that the LPV model is more dependable overall and can help to circumvent locally inaccurate models. In view of this observation, a better result may be obtainable if only the most accurate local models are used for estimation, rather than a random selection among the models available.

The LPV model is accurate and scalable, and hence brings a significant improvement compared to the use of a single average model. Fig. 17 highlights that the LPV model consistently achieves a higher accuracy than the average model, in both estimation and validation conditions (cf. also the output examples in Figs. 14 and 15). While the differences are of a small magnitude, it is important to consider that the scale of the entire problem is small, as discussed in Sec. III. On the one hand, this implies that seemingly negligible changes may have a significant effect. On the other hand, the achievable accuracy in terms of modelling and especially data acquisition is limited and may be close in magnitude to the changes being modelled. Even small errors in the local models are for instance significant given the small global variation to be modelled. Similarly, the small scale emphasises the effect of inaccuracies in the scheduling. Indeed, it can be remarked that although the LPV scheduling is effective overall and yields results (parameters and eigenvalues) significantly closer to the local results than the average model (cf. Secs. V.B and refsec: results dynamics), the difference in the resulting output is less noticeable. It appears that the modelling errors involved are large enough to affect the final result, even though per se they appear to be small, and all the main trends are replicated accurately by the LPV model.

Bearing these points in mind, an average model may be a sufficiently accurate approximation for some applications, if a limited operating domain is considered. Overall, however, the LPV model is more accurate and offers several advantages over both the average model and the set of local models. Unlike the average model, the LPV model does not deteriorate in accuracy as the flight conditions change. Figs. 17 and 18 show that in the central part of the flight envelope the LPV and average model results are very similar, but that the average model increasingly loses accuracy at flight conditions increasingly different from those in the middle of the envelope. This can also be observed in the output (Fig. 14): especially at low velocities, the discrepancy between average model and flight data is clearly visible. This effect will become more pronounced if a wider flight envelope is considered (e.g. through changes to the vehicle configuration, cf. Sec. II.A). Hence, an average model is not a robust solution, and is inadequate for high-accuracy applications.

By contrast, the LPV model retains a similar performance throughout the domain considered, with the exception of isolated outliers, whose decreased performance can be traced back to the estimation data. It is more accurate than the average model and represents a scalable solution that can be extended to cover a vaster flight envelope. The developed model can also be used effectively to predict how the dynamics of the system change, which is not possible with an average model (cf. Fig. 13 and Sec. V.C). While less accurate than the local models – as expected, since the estimation process minimises the difference between LPV model and closest local model –, the LPV model has the advantages of higher flexibility, continuous coverage and a smaller overall model size (a total of 25 parameters, as opposed to 12 parameters per flight condition). Another benefit is that, whereas single local models may be inaccurate, e.g. due to inaccurate identification data, if the majority of the original local models are accurate, the LPV model can bypass local errors (e.g. single outliers) in favour of the more significant overall trends.

The modelling approach itself is therefore considered an effective and useful approach when dealing with flapping-wing vehicles that can be locally represented by LTI models (the most widespread formulation in the literature). Whether the suggested approach remains effective when considering more significant variation (e.g. including the effect of CG shifts, which would allow for considerably higher velocities) must be verified, however the approach remains theoretically applicable. Moreover, the fact that the LPV model remains accurate at the edges of the considered region suggests that some degree of further extrapolation could be handled. The benefits of using a global model as opposed to a rough single average approximation would become more evident if more significant changes were considered. Further, the currently observed effects may become more clearly discernible and easier to model if more accurate and informative data are used.

**Table 5:** Percentage of cases (flight conditions the models are evaluated at) where the LPV model has a better performance than the average and local models, respectively.

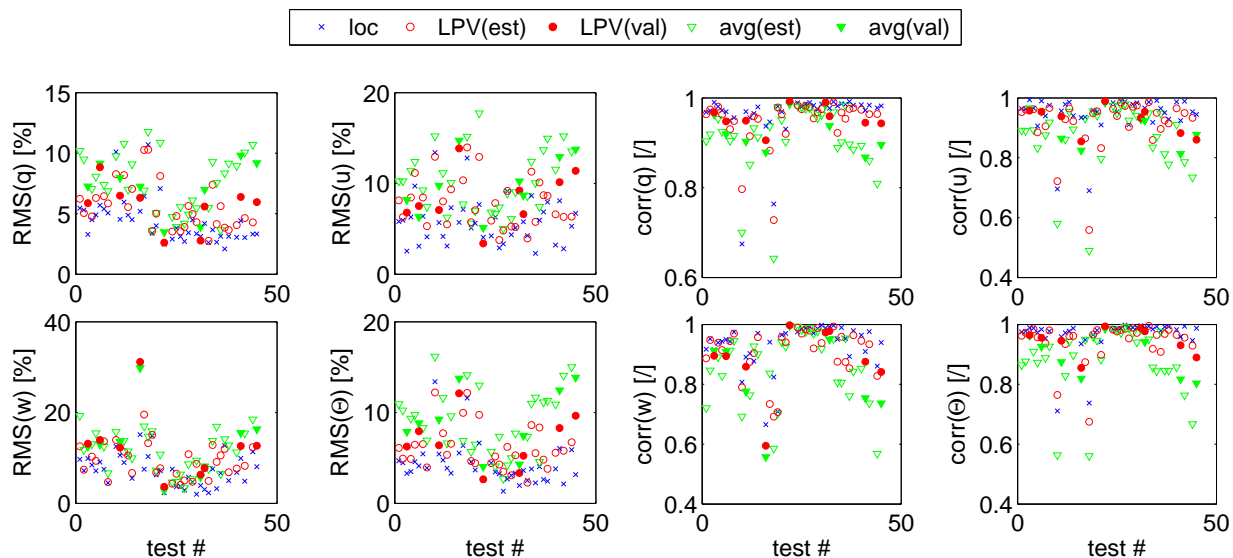| | RMSE: % cases better than | | | | corr: % cases better than | | | |
|---|---|---|---|---|---|---|---|---|
| State | Avg.(est.) | Loc.(est.) | Avg.(val.) | Loc.(val.) | Avg.(est.) | Loc.(est.) | Avg.(val.) | Loc.(val.) |
| $q$ | 87 | 10 | 100 | 11 | 84 | 6 | 100 | 11 |
| $u$ | 81 | 6 | 89 | 11 | 77 | 6 | 67 | 11 |
| $w$ | 81 | 10 | 44 | 0 | 77 | 13 | 67 | 11 |
| $\Theta$ | 84 | 10 | 100 | 0 | 81 | 16 | 100 | 0 |



**Figure 16:** LPV, average and local model-obtained results, compared to flight test data.
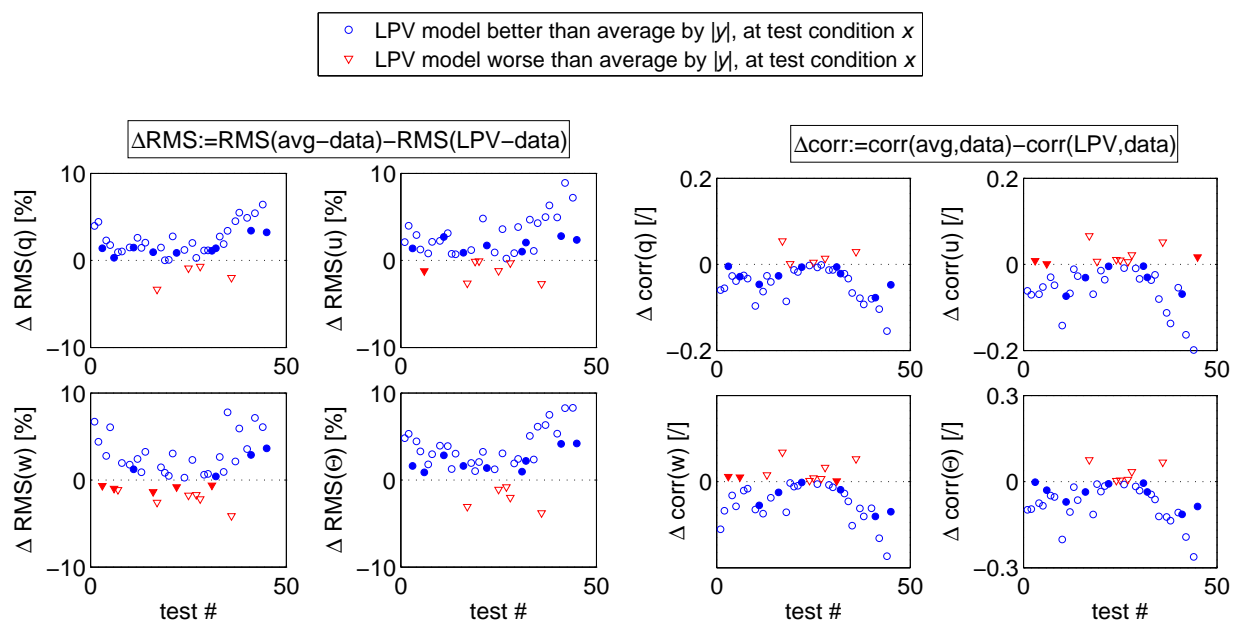


**Figure 17: LPV and average** model-obtained results, compared to flight data (validation sets as filled markers)

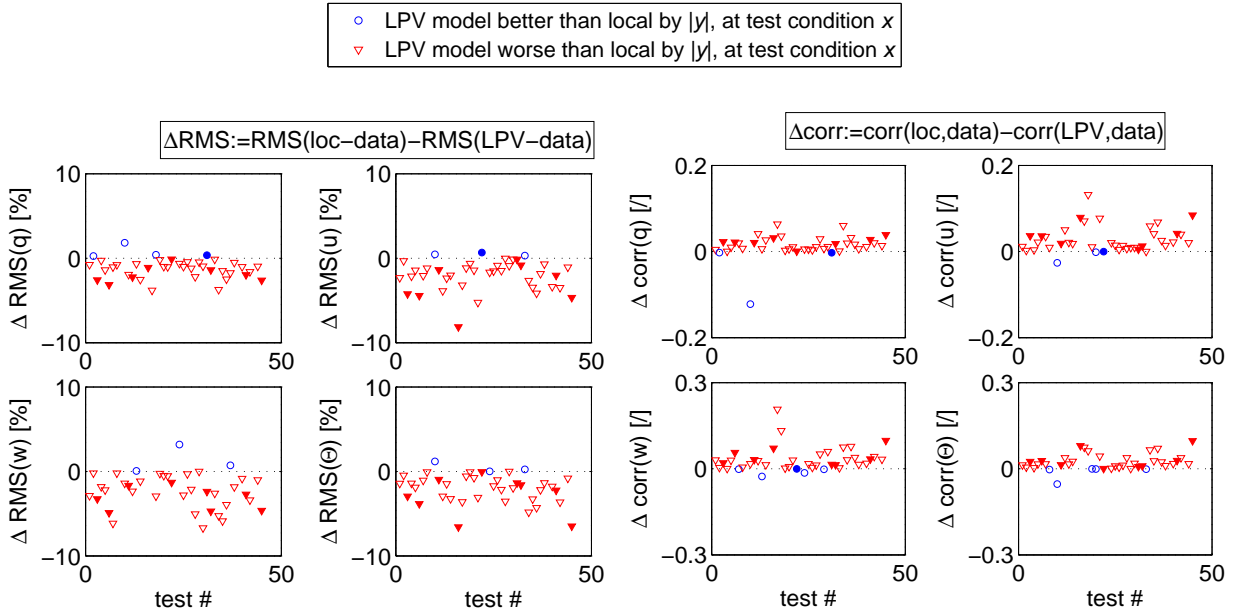American Institute of Aeronautics and Astronautics

**Figure 18: LPV and local** model-obtained results, compared to flight test data (validation sets as filled markers).

# VI.   Conclusions

A linear parameter-varying (LPV) model identification approach was developed to represent the time-averaged dynamics of a flapping-wing micro aerial vehicle (FWMAV). This involved, firstly, estimating local dynamic models of the system, using 46 sets of free-flight data collected in different flight conditions, and, secondly, determining a set of scheduling functions to express the dependency of these models on the flight condition they represent. Results show that the obtained scheduling functions accurately model the key dynamic properties of the vehicle, and therefore constitute a useful means of predicting the system dynamics and simulating the system response in different flight conditions. With a significantly lower number of parameters, the global model achieves an only slightly lower accuracy than the initial set of local models, while additionally providing continuous coverage across the entire range of conditions considered, and therefore also increased flexibility. Furthermore, the model retains an approximately constant accuracy also at the edges of the covered flight envelope, suggesting that some extrapolation is possible and that the approach may be an effective solution also to represent more significant global variation, provided that linear models remain effective locally. The small physical scale of the FWMAV modelling problem was found to be a challenge, as the changes being modelled are significant for the *micro* air vehicle studied, but simultaneously close in magnitude to the error in the data acquisition and modelling process. In spite of this limitation, the modelling approach is promising, and yielded a global model that is accurate but requires few measurements, is computationally light and is easily interpretable. All of these properties make the resulting model highly suitable for simulation and control work. The modelling process also yielded more in depth information on the dynamic properties of the test platform, clearly showing that these vary with the angle of attack and flight velocity and providing insight into how they vary. The observed trends are consistent with flight experience, providing further corroboration of the obtained results. Improved results may be obtainable with more informative and extensive data, leading to more accurate local models and a reduced error in the global modelling process. Furthermore, the suggested approach is considered applicable to account for different vehicle configurations in a single model. This type of extension of the model would likely involve larger changes and therefore more fully exploit the LPV approach.

# References

[1] Ellington, C. P., "The Aerodynamics of Hovering Insect Flight. I. The Quasi-Steady Analysis," *Philosophical Transactions of the Royal Society B: Biological Sciences*, Vol. 305, No. 1122, Feb. 1984, pp. 1–15.

[2] Ellington, C. P., van den Berg, C., Willmott, A. P., and Thomas, A. L. R., "Leading-edge vortices in insect flight,"

*Nature*, Vol. 384, 1996, pp. 626–630.

   [3]Sane, S. P., "The aerodynamics of insect flight," *Journal of Experimental Biology*, Vol. 206, No. 23, Dec. 2003, pp. 4191–4208.

   [4]Dickinson, M. H., Lehmann, F.-O., and Sane, S. P., "Wing Rotation and the Aerodynamic Basis of Insect Flight," *Science*, Vol. 284, No. 5422, June 1999, pp. 1954–1960.

   [5]Taylor, G. K. and Thomas, A. L. R., "Dynamic flight stability in the desert locust Schistocerca gregaria," *Journal of Experimental Biology*, Vol. 206, No. 16, Aug. 2003, pp. 2803–2829.

   [6]Nakata, T., Liu, H., Tanaka, Y., Nishihashi, N., Wang, X., and Sato, A., "Aerodynamics of a bio-inspired flexible flapping-wing micro air vehicle," *Bioinspiration & Biomimetics*, Vol. 6, 2011.

   [7]Grauer, J., Ulrich, E., Hubbard, J. E., Pines, D., and Humbert, J. S., "Testing and System Identification of an Ornithopter in Longitudinal Flight," *Journal of Aircraft*, Vol. 48, No. 2, March 2011, pp. 660–667.

   [8]Caetano, J. V., de Visser, C. C., de Croon, G. C. H. E., Remes, B., De Wagter, C., and Mulder, M., "Linear Aerodynamic Model Identification of a Flapping Wing MAV Based on Flight Test Data," *International Journal of Micro Air Vehicles*, 2013, pp. 1–15.

   [9]Armanini, S. F., de Visser, C. C., and de Croon, G. C. H. E., "Black-box LTI Modelling of Flapping-wing Micro Aerial Vehicle Dynamics," *AIAA Atmospheric Flight Mechanics Conference*, 2015.

   [10]Berman, G. J. and Wang, Z. J., "Energy-minimizing kinematics in hovering insect flight," *Journal of Fluid Mechanics*, Vol. 582, June 2007, pp. 153–168.

   [11]Orlowski, C. T. and Girard, A. R., "Averaging of the Nonlinear Dynamics of Flapping Wing Micro Air Vehicles for Symmetrical Flapping," *AIAA Aerospace Sciences Meeting including the New Horizons Forum and Aerospace Exposition*, 2011.

   [12]Khan, Z. A. and Agrawal, S. K., "Force and moment characterization of flapping wings for micro air vehicle application," *American Control Conference*, 2005, pp. 1515–1520.

   [13]Xiong, Y. and Sun, M., "Stabilization control of a bumblebee in hovering and forward flight," *Acta Mechanica Sinica*, Vol. 25, No. 1, 2009, pp. 13–21.

   [14]Wu, J. and Sun, M., "Control for going from hovering to small speed flight of a model insect," *Acta Mechanica Sinica*, Vol. 25, No. 3, 2009, pp. 295–302.

   [15]Finio, B. M., Perez-Arancibia, N. O., and Wood, R. J., "System identification and linear time-invariant modeling of an insect-sized flapping-wing micro air vehicle," *2011 IEEE/RSJ International Conference on Intelligent Robots and Systems*, 2011, pp. 1107–1114.

   [16]Duan, H. and Li, Q., "Dynamic model and attitude control of Flapping Wing Micro Aerial Vehicle," *IEEE International Conference on Robotics and Biomimetics (ROBIO)*, Dec. 2009, pp. 451–456.

   [17]Chand, A. N., Kawanishi, M., and Narikiyo, T., "Parameter Estimation for the Pitching Dynamics of a Flapping-Wing Flying Robot," *IEEE International Conference on Advanced Intelligent Mechatronics (AIM)*, 2015, pp. 1552–1558.

   [18]Armanini, S. F., de Visser, C. C., de Croon, G. C. H. E., and Mulder, M., "Time-varying model identification of flapping-wing vehicle dynamics using flight data," *Journal of Guidance, Control, and Dynamics*, Vol. 39, No. 3, 2016, pp. 526–541.

   [19]de Croon, G. C. H. E., Perçin, M., Remes, B. D. W., Ruijsink, R., and De Wagter, C., *The DelFly Design, Aerodynamics, and Artificial Intelligence of a Flapping Wing Robot*, Springer Netherlands, 2016.

   [20]Sename, O., Gáspár, P., , and Bokor, J., editors, *Robust Control and Linear Parameter Varying Approaches*, Lecture Notes in Control and Information Sciences, Springer, Berlin Heidelberg, 2013.

   [21]Tóth, R., Van den Hof, P. M. J., Ludlage, J. H. a., and Heuberger, P. S. C., "Identification of nonlinear process models in an LPV framework," *Proceedings of the 9th International Symposium on Dynamics and Control of Process Systems*, , No. Dycops, 2010, pp. 869–874.

   [22]Leith, D. J. and Leithead, W. E., "Survey of Gain-Scheduling Analysis and Design," *International Journal of Control*, Vol. 73, No. 11, 2000, pp. 1001–1025.

   [23]Fujimori, A. and Ljung, L., "Model identification of linear parameter varying aircraft systems," *IMechE Part G: J. Aerospace Engineering*, Vol. 220, 2006.

   [24]Marcos, A. and Balas, G., "Linear parameter varying modeling of the Boeing 747-100/200 longitudinal motion," *AIAA Guidance, Navigation, and Control Conference and Exhibit*, , No. August, 2001, pp. 1–30.

   [25]Marcos, A. and Balas, G. J., "Development of Linear-Parameter-Varying Models for Aircraft," *Journal of Guidance, Control, and Dynamics*, Vol. 27, No. 2, 2004, pp. 218–228.

   [26]Marcos, A., Veenman, J., and Scherer, C. W., "Application of LPV Modeling, Design and Analysis Methods to a Re-entry Vehicle," Tech. Rep. 2011, 2010.

   [27]Balas, G. J., Fiahlo, I., Packard, A., Renfrow, J., and Mullaney, C., "On the Design of the LPV Controllers for the F-14 Aircraft Lateral-Directional Axis During Powered Approach," *American Control Conference*, 1997.

   [28]Seiler, P., Balas, G., and Packard, A., "Linear parameter varying control for the X-53 active aeroelastic wing," *AIAA Atmospheric Flight Mechanics Conference*, 2011.

   [29]Westermayer, C., Schirrer, A., Hemedi, M., and Kozek, M., "Linear parameter-varying control of a large blended wing body flexible aircraft," *IFAC Proceedings*, Vol. 43, 2010, pp. 19–24.

   [30]Weilai, J., Chaoyang, D., and Qing, W., "A systematic method of smooth switching LPV controllers design for a morphing aircraft," *Chinese Journal of Aeronautics*, Vol. 28, No. 6, 2015, pp. 1640–1649.

   [31]Klein, V. and Morelli, E. A., *Aircraft System Identification: Theory And Practice*, AIAA Education Series, Reston, VA, 2006.

   [32]de Croon, G. C. H. E., de Clercq, K. M. E., Ruijsink, R., Remes, B. D. W., and de Wagter, C., "Design, aerodynamics, and vision-based control of the DelFly," *International Journal of Micro Air Vehicles*, Vol. 1, No. 2, 2009, pp. 71–98.

   [33]Armanini, S. F., Karásek, M., E., d. G. C. H., and de Visser, C. C., "Onboard/ offboard sensor fusion for high-fidelity flapping-wing robot flight data," *Journal of Guidance, Control and Dynamics*, Vol. 40, No. 8, 2017.

[34]Armanini, S. F., Karásek, M., de Visser, C. C., de Croon, G. C. H. E., and Mulder, M., "Flight testing and preliminary analysis for global system identification of ornithopter dynamics using on-board and off-board data," *AIAA Atmospheric Flight Mechanics Conference*, 2017.

[35]Karásek, M., Koopmans, A. J., Armanini, S. F., Remes, B. D. W., and de Croon G. C. H. E., "Free Flight Force Estimation of a 23.5 g Flapping Wing MAV using an on-board IMU," *International conference on intelligent robots and systems (IROS)*, 2016.

[36]Caetano, J. V., de Visser, C. C., Remes, B. D., De Wagter, C., Van Kampen, E.-J., and Mulder, M., "Controlled Flight Maneuvers of a Flapping Wing Micro Air Vehicle: a Step Towards the Delfly II Identification," *AIAA Atmospheric Flight Mechanics Conference*, 2013.

[37]Orlowski, C., Girard, A., Shyy, W., and Arbor, A., "Derivation and simulation of the nonlinear dynamics of a flapping wing micro-air vehicle," .

[38]Bolender, M. A., "Rigid Multi-Body Equations-of-Motion for Flapping Wing MAVs using Kane Equations," *AIAA Guidance, Navigation, and Control Conference*, No. 2009-6158, Aug. 2009.

[39]Grauer, J. A., Hubbard, J. E., and Jr, J. E. H., "Multibody Model of an Ornithopter," *Journal of Guidance, Control, and Dynamics*, Vol. 32, No. 5, Sept. 2009, pp. 1675–1679.

[40]Sun, M. and Xiong, Y., "Dynamic flight stability of a hovering bumblebee." *Journal of Experimental Biology*, Vol. 208, No. Pt 3, Feb. 2005, pp. 447–59.

[41]Faruque, I. and Sean Humbert, J., "Dipteran insect flight dynamics. Part 1 Longitudinal motion about hover." *Journal of theoretical biology*, Vol. 264, No. 2, May 2010, pp. 538–52.

[42]Mulder, J., *Design and evaluation of dynamic flight test manoeuvres*, Phd, 1986.

[43]Morelli, E., "Flight test validation of optimal input design and comparison to conventional inputs," *AIAA Atmospheric Flight Mechanics Conference*, 1997.

[44]Papageorgiou, G., Glover, K., D'Mello, G., and Patel, Y., "Taking robust LPV control into flight on the VAAC Harrier," *Proceedings of the 39th IEEE Conference on Decision and Control*, Vol. 5, 2000, pp. 4558–4564 vol.5.

[45]Hammoudi, M. N. and Lowenberg, M. H., "Dynamic gain scheduled control of an F16 model," *AIAA Guidance, Navigation and Control Conf.*, 2008.

[46]Bamieh, B. and Giarré, L., "Identification of linear parameter varying models," *International Journal of Robust and Nonlinear Control*, Vol. 12, No. 9, 2002, pp. 841–853.

[47]Toth, R., *Modeling and Identification of Linear Parameter-Varying Systems an Orthonormal Basis Function Approach*, Phd thesis, Delft University of Technology, 2008.

[48]Marcos, A. and Bennani, S., "LPV modeling, analysis and design in space systems: Rationale, objectives and limitations," *AIAA Guidance, Navigation, and Control Conference and Exhibit*, , No. August, 2009, pp. 1–23.

[49]Jategaonkar, R., *Flight Vehicle System Identification A Time Domain Methodology*, AIAA Progress in Astronautics and Aeronautics, Reston, VA, USA, 2006.

[50]Klein, V. and Batterson, J. G., "Determination of airplane model structure from flight data using splines and stepwise regression," Tech. Paper 2126, NASA, 1983.

American Institute of Aeronautics and Astronautics